CONFIDENTIAL

UNCLASSIFIED

C2

NACA

RESEARCH MEMORANDUM

A FLIGHT INVESTIGATION OF AREA-SUCTION AND BLOWING BOUNDARY-LAYER CONTROL ON THE TRAILING-EDGE FLAPS OF A 35° SWEPT-WING CARRIER-TYPE AIRPLANE

By Hervey C. Quigley, Francis W. K. Hom,
and Robert C. Innis

Ames Aeronautical Laboratory
Moffett Field, Calif.

CLASSIFICATION CHANGED
To UNCLASSIFIED

By authority of TPA #33 Date 10-28-60
ER6

LIBRARY COPY
APR 29 1957
LANGLEY AERONAUTICAL LABORATORY
LIBRARY, NACA
LANGLEY FIELD, VIRGINIA

CLASSIFIED DOCUMENT

This material contains information affecting the National Defense of the United States within the meaning of the espionage laws, Title 18, U.S.C., Secs. 793 and 794, the transmission or revelation of which in any manner to an unauthorized person is prohibited by law.

NATIONAL ADVISORY COMMITTEE
FOR AERONAUTICS
WASHINGTON
April 22, 1957

CONFIDENTIAL

UNCLASSIFIED

NASA Technical Library
3 1176 01434 9378

UNCLASSIFIED

NATIONAL ADVISORY COMMITTEE FOR AERONAUTICS

RESEARCH MEMORANDUM

A FLIGHT INVESTIGATION OF AREA-SUCTION AND BLOWING BOUNDARY-LAYER CONTROL ON THE TRAILING-EDGE FLAPS OF A 35° SWEPT-WING CARRIER-TYPE AIRPLANE

By Hervey C. Quigley, Francis W. K. Hom, and Robert C. Innis

SUMMARY

Flight tests were conducted on an FJ-3 airplane to determine the flight characteristics of a carrier-type airplane with area-suction and with blowing boundary-layer control on the trailing-edge flaps. Measurements were made of the lift and drag for the airplane with both types of boundary-layer control in conjunction with slatted and extended cambered wing leading edges. Measurements were made also of the bleed-air requirements for the two flap boundary-layer control systems. Flight evaluations were made of the stall and approach characteristics of the airplane for the various wing leading-edge and flap configurations. Computations were made to show the effect of boundary-layer control on the take-off and landing performance.

The results showed that the blowing boundary-layer control on the flaps deflected 55° gave flap lift increments of 0.53 to 0.59 (depending on the leading-edge and nozzle configuration) as compared to 0.42 for the area-suction type and 0.34 for the standard 45° slotted flap for the landing-approach configuration (12° angle of attack, 85-percent engine rpm). The maximum lift coefficients were consistently higher with the blowing flap than with the suction flap when equal amounts of engine bleed air were used for each leading-edge device tested. Computation showed the landing and take-off performance was improved by both suction and blowing on the flap compared to the 45° slotted flap, but the larger gains were with the blowing flap. The field carrier-landing approach speeds were reduced an average of 2 knots with the suction flap and 10 knots with the blowing flap. All the pilots' approach speeds were within 3 knots of 1.125 stall speed.

CONFIDENTIAL UNCLASSIFIED

INTRODUCTION

The landing-approach and catapult take-off speeds of carrier-type aircraft have increased as operational speeds increased. One of the promising methods of reducing these approach and catapult take-off speeds is the application of boundary-layer control to the trailing-edge flaps. Since relatively high engine powers are required for carrier landing approaches, a boundary-layer control system utilizing engine bleed air is well adapted to carrier airplanes.

In the flight tests of an F9F-4 airplane (ref. 1) with wing-shroud-blowing boundary-layer control on the trailing-edge flaps, and an F-86A (refs. 2 and 3) with area-suction boundary-layer control on the trailing-edge flaps, it was found that the landing-approach speeds in field carrier-landing approaches were reduced appreciably. Since the F9F-4 had shown improved landing and catapult performance in actual carrier operation (ref. 4), interest was focused on testing a representative carrier-type swept-wing airplane with boundary-layer control flaps. The Bureau of Aeronautics, Navy Department, assigned an FJ-3 to the NACA. The NACA was to install an area-suction flap and flight test the airplane to determine the low-speed aerodynamic characteristics.

At the time the initial flight tests were being conducted with the area-suction flap on the FJ-3, a blowing boundary-layer control system was flight tested on the F-86F (ref. 5). The lift values obtained by blowing over the flaps were considerably larger than those obtained on the F-86A and the FJ-3 with area suction. Because it appeared that greater lift gains, and therefore more reduction in approach speeds, might be possible with a blowing system, an additional set of flaps employing blowing boundary-layer control was constructed for the FJ-3 airplane. The suction and blowing flaps were readily interchangeable and offered a convenient comparison of the relative merits of the two systems.

Flight tests were conducted with the area-suction flap with both perforated and sintered porous material, and with the blowing flap with two nozzle sizes. Since the maximum lift obtainable was anticipated to be dependent on wing leading-edge separation, both the suction and blowing flaps were tested in conjunction with the slatted and the extended cambered leading edges currently used on FJ-3 airplanes. The airplane with both types of boundary-layer control systems was evaluated by the pilots to determine carrier-type landing-approach and stalling characteristics. Computations of the performance characteristics were made from measured values of lift, drag, and engine thrust. The results of the flight tests and the computations are reported herein.

NOTATION

b	wing span, ft
BLC	boundary-layer control
C_D	drag coefficient, $\frac{D}{qS}$
C_L	lift coefficient, $\frac{L}{qS}$
ΔC_L	increment of lift due to flaps
$C_{L_{max}}$	maximum lift coefficient
C_Q	flow coefficient, $\frac{Q}{V_\infty S}$
C_μ	momentum coefficient, $\frac{w/g}{qS} V_j$
D	drag, lb
g	acceleration of gravity, 32.2 ft/sec^2
h	nozzle height, in.
L	lift, lb
L.E.	leading edge
p	free-stream static pressure, lb/ft^2
p_d	engine bleed air total pressure in flap duct, lb/ft^2
p_f	flap plenum-chamber pressure, lb/ft^2
C_{p_f}	flap plenum-chamber pressure coefficient, $\frac{p_f - p}{q}$
p_T	duct total pressure, lb/ft^2
q	free-stream dynamic pressure, lb/ft^2

Q	volume of air removed through porous material, cu ft/sec
S	wing area, sq ft
T	engine thrust, lb
V_a	landing-approach velocity, knots
ΔV_a	reduction in landing-approach velocity due to boundary-layer control, knots
V_j	velocity of blowing jet assuming isentropic expansion, ft/sec
V_∞	free-stream velocity, ft/sec
V_S	stalling velocity, knots
ΔV_S	reduction in stalling velocity due to boundary-layer control, knots
w	weight flow of air, lb/sec
W	gross weight of airplane
α	angle of attack, deg
δ_f	flap deflection normal to flap hinge line, deg
μ	friction coefficient
ρ	mass density of air, slugs/cu ft

EQUIPMENT AND TESTS

Airplane and Boundary-Layer Control Flaps

Airplane.- The tests were conducted with an FJ-3 airplane. A two-view drawing and a photograph of the airplane are presented in figures 1 and 2, respectively. The geometric data for the airplane are given in table I.

The following modifications were made to the airplane to incorporate the area-suction and the blowing boundary-layer control systems. The wing shroud ahead of the flap was rebuilt to accommodate the nose section of the boundary-layer control flap. A manifold was installed on the J65-W-4 engine to collect the air from the bleed ports of the last stage of the engine compressor. A pilot-controlled valve was installed

in the ducting between the engine and the flaps to control the flow of bleed air; the valve was fully open for all boundary-layer control tests. Two-inch ducting was routed internally from the valve to a rotating O-ring seal at the flap center of rotation. The ducting and the control valve weighed 17-1/2 pounds. The flaps were plain type with the hinge line at the lower surface. Two sets of flaps, one with area-suction and the other with blowing boundary-layer control, were constructed by modifying standard FJ-3 slotted flaps. The suction and blowing flaps weighed 45 and 38 pounds, respectively, more than the standard FJ-3 flaps.

Suction flap.- Figure 3 is a photograph of one of the area-suction flaps. Figure 4 is a typical cross section of the flap showing an ejector pump. Twenty-two (11 in each flap) ejector pumps were used for the suction source. The ejector pumps were designed to operate most efficiently at 85-percent engine rpm (assumed landing-approach rpm) using pump data from reference 6. Figure 5(a) is a close-up view of the suction flap with one section of the sintered porous material removed to show the primary air tube and the ejector nozzles. Figure 5(b) shows a close-up view of a few of the diffuser exits on the lower surface of the flap.

Two types of porous material, sintered stainless steel and perforated aluminum, were tested on the flap radius. Figure 6 is a close-up view of the suction flap with the perforated porous material. The design flow characteristics used for both types of porous material are shown in figure 7. Sintered porous panels were used for all the tests with the slatted wing leading edge; perforated panels were used for all the tests with the extended cambered leading edge except for a brief test to compare the effects of the two types of porous material. The performance of the ejector pumps with the two types of porous material on the flap is shown in figure 8. The difference in pressure drop through the porous material with inflow velocity, as discussed in reference 7, accounts for the difference in the variation of secondary pressure ratio with primary pressure ratio for the two materials.

Blowing flap.- A close-up view of the blowing-type boundary-layer control flap is shown in figure 9, and figure 10 is a sketch of the cross section of the flap showing the primary air tube and the nozzle. The nozzle was continuous (no spacers) over the span of the flap. Two nozzle gaps were tested: a nominal 0.01-inch gap (nozzle area 0.0142 sq ft), and a nominal 0.02-inch gap made by installing a 0.01-inch shim under the nozzle block (nozzle area 0.0264 sq ft).

Bleed air.- Figure 11 shows the primary pressure ratio variation with engine rpm. The data indicate that with the larger blowing nozzle the pressure ratio was lower due to duct losses than with the smaller blowing nozzle and the ejector pump. The jet velocity was sonic above approximately 60-percent engine speed.

The amount of engine bleed air used at various engine speeds for the two blowing nozzles and the ejector pumps is shown in figure 12. The flow quantities were calculated from measurements of calibrated total and static pressure and temperature in the ducting between the valve and the flap. The area of the ejector pump nozzles and the 0.01-inch blowing nozzle was the same; therefore, the primary pressure ratio and weight flow of bleed air were about the same for a given engine speed.

The thrust of the engine with and without extracting bleed air is shown in figure 13. These data were obtained on a thrust stand with the flaps deflected 65° and include the thrust effects of the blowing nozzle and the ejector pump exits. The blowing flap with the 0.02-inch nozzle gap resulted in a 4-percent thrust loss at 100-percent engine speed.

Wing leading edges.- Flight tests were conducted with both a slatted leading edge used in early versions of the airplane, and the extended cambered leading edge with fence currently used on FJ-3 airplanes. The fence was a 25-percent-chord, leading-edge, wrap-around type at 61-percent wing semispan. Tests were also made with the following adaptations of the two standard leading edges: (a) slats locked closed and sealed, (b) extended cambered leading edge without fence, and (c) slats operating but with an NACA 23012 cambered section from the inboard edge of the slat to the fuselage, hereinafter called the slatted leading edge with modified inboard section. Figure 14 shows cross-sectional sketches of the various leading-edge configurations.

Instrumentation and Tests

Instrumentation.- Standard NACA instruments were used to record airspeed, altitude, acceleration, angle of attack, and duct pressure and temperature. The angle of attack was determined by a vane 9 feet in front of the nose of the airplane. Free-stream total and static pressures were taken from an NACA swiveling airspeed head mounted on the end of a nose boom 10 feet long. Duct pressures and temperatures were measured in the ducting between the control valve and the flap.

Tests.- All tests were made with the wing sealed (except for a brief test to show the effect of sealing). Sealing was accomplished by taping all openings in the wing through which air might percolate, such as the leading-edge hinges, wing fold line, and the wing-fuselage juncture. All the data presented herein are for the wing-sealed condition.

The underwing fuel tanks were removed for all tests reported herein.

The flight tests were conducted at approximately 5000 feet altitude over a speed range from 170 knots to the stall to determine the aerodynamic characteristics. The average wing loading and center of gravity for the tests were 50 pounds per square foot and 0.24 mean aerodynamic chord, respectively. The airplane was tested with flap deflections of 0°, 35°, 45°, 55°, and 65°.

The stall and field carrier-landing approach characteristics were determined by Ames pilots using the procedure outlined in reference 5. The landing-approach evaluations were made at Crows Landing Auxiliary Landing Field (elevation 165 ft) with the aid of either a Navy landing signal officer or the landing-approach mirror.

RESULTS AND DISCUSSION

Lift and Drag Characteristics

The effect of boundary-layer control.- The lift and drag characteristics are presented in figure 15 for the airplane with and without area-suction and with and without blowing boundary-layer control on the trailing-edge flaps. The data for the airplane with the flaps deflected are for the configuration found to be optimum for carrier-type landing approaches, that is, 55° flap deflection, landing-gear down, and dive brakes closed. The data in 15(a) are for the airplane with a slatted leading edge, and in 15(b) for the airplane with the extended cambered leading edge with fence. The lift and drag data for the basic airplane with the 45° slotted flaps are also shown in figure 15(a) for comparative purposes. It can be seen from these data that the maximum lift coefficient and the flap lift effectiveness, ΔC_L, were increased with both types of boundary-layer control as compared to the airplane with the 45° slotted flap. The maximum lift coefficient was 0.05 higher with the area-suction flap and 0.17 higher with the blowing flap than for the airplane with 45° slotted flaps. The small difference in the lift curves for the suction and blowing flaps with boundary-layer control off was believed due to outflow through the porous material of the suction flap decreasing the flap lift.

The variation of the flap lift with angle of attack is shown in figure 16 for the various configurations. These data show that at an angle of attack of 12° (assumed approach attitude) blowing on the flap more than doubled the lift effectiveness of the plain flap, while suction improved it about 60 percent.

The flap lift variation with flap angle for $\alpha=12^{\circ}$, shown in figure 17, indicates that above 55° flap deflection the flap lift improves very little with flap deflection with either type of boundary-layer control. Theoretical flap lift increments as predicted from reference 8 were achieved with the larger nozzle blowing flap at flap deflections of 35° and 45°.

The drag data of figure 15 show that at the lower lift coefficients the drag is increased due to boundary-layer control while at the higher C_L values the drag is decreased. This is consistent with previous boundary-layer control investigations (refs. 3, 5, 9, and 10) and had little effect on the operation of the airplane.

The effect of wing leading-edge configuration.- Early in the tests of the boundary-layer control flaps with the slatted leading edge it was noted that the increased flap lift due to boundary-layer control was reduced near $C_{L_{max}}$ (fig. 15(a)). This was especially true for the area-suction flap for which the lift increment due to suction was 0.17 at $\alpha=12^{\circ}$ and only 0.05 at $C_{L_{max}}$. Tuft studies of the air flow over the wing showed that as $C_{L_{max}}$ was approached, separation started at the leading edge of the wing inboard of the slats and spread back over the flap and outboard at the stall. To study further the effect of the leading edge on the lift with boundary-layer control flaps, tests were made with several other leading-edge configurations.

To determine if the discontinuity of the inboard edge of the slat contributed to the shape of the lift curve and lift increment due to suction, the airplane was flown with the slats locked closed and sealed. The lift data, figure 18(a), showed that the lift curves with the slats open and closed were essentially the same up to $C_{L_{max}}$ with slats closed.

In an attempt to delay the separation inboard of the slats at the high angles of attack, the leading edge between the inboard edge of the slats and the fuselage was modified as shown in figure 14(c). The lift curves, figure 18(b), showed that with the modified leading edge the linear portion of the lift curves was extended to a higher angle of attack and $C_{L_{max}}$ was increased. Since the $C_{L_{max}}$ for boundary-layer control off was also improved, there was little gain in lift due to boundary-layer control at $C_{L_{max}}$. Tuft studies showed that as angle of attack was increased, separation started at the trailing edge near the wing tip, followed by separation inboard of the slat. A pitch-up which the pilots considered unsatisfactory occurred at about 3 knots above normal stall speed. In accelerated stalls in turning flight the pitch-up was less severe and was considered acceptable; however, the airplane had a tendency to roll out of the turn.

The results of the flight tests with the extended cambered leading edge with and without the fence are given in figure 18(c). The data show that the fence did not affect the flap lift; however, the fence reduced $C_{L_{max}}$ by 0.10 for both the suction- and blowing-flap configurations. The abrupt roll-off experienced by the pilots at the stall was slightly reduced with the fence.

The following table summarizes the flap lift increments and maximum lift coefficients obtained at 85-percent engine speed and 55° flap deflection for all the leading edges tested.

Leading-edge configuration	ΔC_L (α=12°)		$C_{L_{max}}$	
	Suction	Blowing (h=0.01 in.)	Suction	Blowing (h=0.01 in.)
Slats open	0.42	0.57	1.43	1.55
Slats closed	.42	---	1.34	---
Slats open with modified inboard section	.42	.55	1.54	1.63
Extended cambered with fence	.42	.53	1.37	1.52
Extended cambered without fence	.42	.53	1.47	1.60

Effect of engine speed on lift.- Since the engine compressor bleed air is used to operate both types of boundary-layer control, the suction of the ejector pumps and the momentum of the blowing nozzle will be a direct function of the engine speed. Therefore, the flap lift increment and the maximum lift coefficient will vary with engine speed with either type of boundary-layer control. It can be seen in figure 19 that the increase in flap lift with engine speed is almost linear for the blowing-flap configurations while the increase is more gradual with little increase above 85-percent engine speed for the suction-flap configurations. Figure 20 shows the same trend for the variation of $C_{L_{max}}$ with engine speed. The greatest variation of $C_{L_{max}}$ with engine speed was obtained with the 0.02-inch nozzle blowing flap and cambered leading edge. In this configuration the $C_{L_{max}}$ varied from 1.37 at 50-percent to 1.63 at 100-percent engine speed. This variation in $C_{L_{max}}$ and engine thrust would mean a change of from 103 to 89 knots in the stalling speed at a gross weight of 15,000 pounds.

Other factors that affect lift.- It was found early in the tests that sealing the openings in the wing through which air might percolate increased the maximum lift, especially for the suction flap. The effect of sealing is shown on the lift curves of figure 21 for the airplane with the slatted leading edge. No attempt was made to determine where on the wing the sealing was most effective.

The effect of the landing gear and dive brakes on the lift and drag of the airplane is shown in figure 22 for the suction flap and the slatted leading edge. The data show that the flap lift was reduced by 0.05 and 0.02 at $\alpha=12^{\circ}$ due to the landing gear and dive brakes, respectively. The $C_{L_{max}}$ was reduced by 0.05 due to the landing gear while the dive brakes had no measurable effect on $C_{L_{max}}$.

Flow Requirements

Suction flap.- The volume of air removed through the porous material was not measured, but the flow coefficient, C_Q, could be estimated from pumping characteristics of the ejector pumps and measured values of pressure ratio. An estimated C_Q value of 0.0005 (the value determined in ref. 9 for flow attachment on a similar configuration) was achieved at pressure coefficients of about -5.5 with the perforated and -7.5 with sintered porous materials. The data in figure 23 show that these values of C_{p_f} occurred at engine speeds of about 85 percent. It can be seen from figures 19 and 23 that only small increases in lift due to suction was achieved at engine speeds above 85 percent. These data indicate that sufficient flow coefficient and pressure coefficient were available to give near maximum suction lift increment during landing approaches.

The difference in flow characteristics of the sintered and the perforated porous materials gave slight differences in lift. It is shown in figure 23 that with the perforated material the lift coefficient at 12° angle of attack is 0.02 higher at 55-percent engine speed but no higher at 100-percent engine speed as compared to the sintered material. The lift curves of the airplane with the suction flap with the two materials are shown in figure 24. These data, at 85-percent engine speed, show that with the perforated material the $C_{L_{max}}$ is 0.025 higher than with the sintered material. These differences in lift characteristics with the two types of porous material are considered small; however, the tests were too limited for a complete comparison of the relative merits of sintered and perforated porous materials for suction flaps.

Blowing flap.- The variation of lift coefficient with momentum coefficient is presented in figure 25 for 8° and 12° angles of attack and for $C_{L_{max}}$. These data show that C_L increased rapidly with C_μ up to a C_μ value of about 0.007 above which the increase in C_L with C_μ was at a much lower rate. It can be seen from figure 25(b) that the variation of C_L with C_μ was the same for both nozzle gaps tested. Wind-tunnel tests of reference 10 indicated the initial increase in lift with C_μ was due primarily to boundary-layer control, while the further increase in C_L was due to increased circulation over the wing. The data in figure 26 show the variation of C_μ with airspeed and engine speed for both the 0.01-inch and the 0.02-inch nozzle gaps. It is shown

by these data that in the landing-approach speed range of 100 to 115 knots a C_μ value of about 0.007 would require 75- to 80-percent engine speed with the 0.01-inch nozzle and only 65 to 70 percent with the 0.02-inch nozzle. Since engine speeds in excess of 80 percent are required for carrier-type approaches, the C_μ values in the present tests were above 0.007.

Performance

Computations were made using measured values of lift, drag, and engine thrust to determine stalling speed, approach speed, landing distance, take-off distance, catapult launching speed, and rate of climb. The methods used for computing performance are noted in the Appendix and are considered to be accurate enough for comparison purposes. The thrust losses due to engine bleed are considered in the computations where applicable.

Stalling speed.- The stalling-speed variation with gross weight is shown in figure 27. The stalling speeds were computed from $C_{L_{max}}$ values and include effects of thrust. These data show that the difference in stalling speed between the suction and blowing flap (h=0.01 in.) is 3 knots with the slatted leading edge and 5 knots with the cambered leading edge. With the large nozzle blowing flap (h=0.02 in.) the stalling speed was 7 knots less than with the suction flap.

Approach speed.- Figure 28 shows the computed variation of approach speed with gross weight. These data were computed on the assumption that the pilot would approach at the same angle of attack and lift coefficient regardless of the gross weight. The following table notes the pilots' average α and C_L used in field carrier-landing approaches.

Configuration leading edge	Flap	Average approach α, deg	Average approach C_L
Slatted	45° slotted	11.4	1.06
↓	55° BLC off	14.5	1.14
	55° suction	12.8	1.19
	55° blowing (h=0.01 in.)	11.3	1.29
Extended cambered	55° BLC off	12.6	1.04
↓	55° suction	10.6	1.11
	55° blowing (h=0.01 in.)	11.0	1.20
	55° blowing (h=0.02 in.)	10.5	1.24

The pilots' opinions of the use of boundary-layer control flaps in the landing approach will be discussed later.

Landing distance.- It can be seen from figure 29 that the computed landing distance is reduced by both types of boundary-layer control. Landing distance for the airplane with the slatted leading edge was reduced about 16 percent with the suction flap and 22 percent with the blowing flap as compared to the standard airplane with the 45° slotted flap. The shortest landing distance computed was for the airplane with the 0.02-inch nozzle blowing flap and with the extended cambered leading edge.

Take-off distance.- The computed take-off distance was reduced by both types of boundary-layer control as shown in figure 30(a). The blowing flap reduced the take-off distance about 9 percent while the reduction with the suction flap was only about 3 percent as compared to the airplane with 45° slotted flaps. The take-off distances with flap deflections of 35°, 45°, 55°, and 65° are shown in figure 30(c) for the extended cambered leading edge and the blowing flap (h=0.02 in.). The data indicate the minimum distances were with the 55° flap deflection; however, the differences in take-off distance with flap deflection are considered small.

Catapult launching.- The computed catapult launching-speed variation with gross weight is shown in figure 31 for various configurations. These data show that with either type of boundary-layer control flap the airplane could be launched heavier at a given catapult end speed and wind over the deck than the basic airplane; with the slatted leading edge the airplane could be launched about 1600 pounds heavier with the blowing flap, and about 600 pounds heavier with the area-suction flap.

Figure 32 shows that the computed rate of climb at the end of the catapult (1.05 V_S) is decreased with both types of boundary-layer control flaps due to the engine thrust loss and higher induced drag. However, all configurations had longitudinal accelerations much greater than 0.065g[1] at the end of the catapult.

Pilots' Opinions

The Ames pilots evaluated the airplane with various leading-edge and flap configurations to determine the stalling speed, stalling characteristics, carrier landing-approach speed, and reason for limiting approach speed. (The evaluation flights were without a rudder pedal shaker for artificial stall warning.) The results of these evaluations have been tabulated in table II. In figure 33 the individual pilot's approach speeds, noted in table II, have been converted to C_L and marked on the lift curves. The pilots' average approach speeds for each configuration evaluated are shown in figure 28.

[1]Assumed minimum acceleration value used to assure that the airplane does not sink after launch.

These data indicate that the pilots used the increased flap effectiveness and maximum lift due to boundary-layer control to reduce their speed in a carrier-type landing approach. The amount the pilots' average approach speeds were reduced varied from 2 knots for the airplane with the suction flap and slatted leading edge to 10 knots with the blowing flap (h=0.02 in.) and cambered leading edge as compared to the basic airplane with the slatted leading edge. Proximity to the stall was the reason given by the pilots for limiting their approach speeds for the majority of the evaluation flights (table II). The exception was the blowing-flap (h=0.01 in.) and the 45° slotted-flap configurations (basic airplane) with the slatted leading edge; for these configurations the pilots limited their approach speeds because of inadequate altitude control.

The stalling characteristics of the airplane were more a function of the leading edge than the flap configuration. With the slatted leading edge the airplane had marginal stall warning and a satisfactory stall, and with the extended cambered leading edge (with fence) the stall was considered by two of the pilots to be unsatisfactory, and by one to be marginal due to the abrupt roll-off at the stall with no stall warning.

Approach-Speed Criteria

Two of the landing-approach criteria suggested in reference 2 for determining minimum comfortable landing-approach speed in carrier-type approaches were stall speed and speed for minimum drag. The relationship of the individual Ames pilot's approach speed to these two criteria for the FJ-3 with the two leading-edge and five flap configurations are shown in figures 34 and 35. In figure 34 it is shown that the pilot approach speeds are within 3 knots of a mean of 1.125 V_S. It is of interest to note that the pilots approached as close to the stall with the extended cambered leading edge as with the slatted leading edge even though the pilots considered the stall with the cambered leading edge unsatisfactory and with the slats satisfactory (table II). It is also of interest to note that minimum comfortable approaches were made as low as 1.10 V_S. The change in pilot's approach speed due to boundary-layer control varies directly (within 3 knots) with the change in stall speed due to boundary-layer control as shown in figure 34. From the landing-approach data for this airplane it appears that the change in approach speed due to different leading-edge and flap configurations was dependent on the change in stall speed.

It is shown in figure 35 that the approach speeds were for most cases less than the speed for minimum drag. The trend seemed to be for the pilot to approach closer to the speed for minimum drag as the approach speeds were reduced.

CONCLUSIONS

The following conclusions have been made from this investigation of area-suction and blowing boundary-layer control on the trailing-edge flaps:

1. The plain-flap effectiveness was increased as much as 100 percent with blowing boundary-layer control and 60 percent with area-suction boundary-layer control on the trailing-edge flaps deflected 55° (considered optimum for carrier-type landing approaches) at 12° angle of attack for the landing-approach configuration of the airplane.

2. The increase in maximum lift coefficient $C_{L_{max}}$ due to boundary-layer control was dependent on the leading-edge configuration. With a 0.01-inch nozzle blowing flap the increase in $C_{L_{max}}$ due to boundary-layer control for the landing-approach configuration of the airplane was 0.13 with the slatted leading edge and 0.23 with the extended cambered leading edge (with fence). Similarly, with the area-suction flap the increase in maximum lift coefficient was 0.05 and 0.09 for the slatted and extended cambered leading edges, respectively.

3. The differences in lift characteristics with the perforated as compared to the sintered porous material on the area-suction flap were small.

4. Computations showed that the landing, take-off, and catapult launching performance would be improved with either blowing or suction boundary-layer control on the flap, while the rate of climb after catapult launching would be less than the basic airplane.

5. The reduction in pilots' approach speeds in field-carrier landing approaches with the boundary-layer control flaps varied from 2 knots for the airplane with the area-suction flap and slatted leading edge to 10 knots with the blowing flap and extended cambered leading edge as compared to the basic airplane with the slatted leading edge.

6. The minimum comfortable pilots' approach speeds in carrier-type landing approaches were within 3 knots of 1.125 stalling speed for all configurations evaluated and were for most cases below the speed for minimum drag.

Ames Aeronautical Laboratory
National Advisory Committee for Aeronautics
Moffett Field, Calif., Feb. 14, 1957

APPENDIX A

METHODS USED FOR PERFORMANCE EVALUATION

The following equations and assumptions were used in computing the performance.

Stall velocity:

$$V_S = \sqrt{\frac{295(W - T \sin \alpha)}{SC_{L_{max}}}}, \text{ knots}$$

where

$$\alpha = \text{angle of attack at } C_{L_{max}}$$

Approach velocity:

$$V_a = \sqrt{\frac{295\ W}{S(C_L + C_D \tan \alpha)}}, \text{ knots}$$

where α, C_L and C_D are for the approach attitude.

Landing distance:

$$\text{Air distance} = \left(\frac{V_{50}^2 - V_L^2}{2g} + 50\right) \frac{L}{D}, \text{ ft}$$

(ref. 11, p. 198) where V_{50} is pilot's actual approach speed in feet per second, and V_L is the landing velocity,

$$V_L = 1.05\ V_S \quad \text{ft/sec}$$

$$\text{Ground run} = \frac{V_L^2}{2g[\mu - (D/L)]} \log_e \left(\frac{L}{D}\right)\mu, \text{ ft}$$

(ref. 12, p. 312) where $\mu = 0.4$

Take-off distance:

$$\text{Ground run} = \frac{WV_{TO}^2}{2g[T - \mu W - Sq(C_D - \mu C_L)]}, \text{ ft}$$

(ref. 11, pp. 195-196)

$$\text{Air distance} = \frac{50\ W}{T-D} + \frac{V_{TO}^2}{g\sqrt{2}},\ \text{ft}$$

(ref. 13, p. 51) where take-off velocity

$$V_{TO} = 1.2\ V_S$$

$$= 1.2\sqrt{\frac{843(W - T \sin \alpha)}{SC_{L_{max}}}},\ \text{ft/sec}$$

$$q = \frac{\rho}{2}(0.7\ V_{TO})^2$$

T = thrust at 100-percent engine speed

α = angle of attack at $C_{L_{max}}$

$\mu = 0.02$

(The assumption is made that steady climb has been reached before attaining the 50-foot height.)

Catapult end speed:

$$V_{TO} = \sqrt{\frac{295(W - T \sin \alpha_{TO})}{SC_{L_{TO}}}},\ \text{knots}$$

where

T = thrust at 100-percent engine speed

$C_{L_{TO}} = 0.9\ C_{L_{max}}$

α_{TO} = angle of attack at $C_{L_{TO}}$

Climb:

$$\text{Rate of climb} = \frac{60\ V_c(T - D)}{W},\ \text{ft/min}$$

where

$V_c = 1.05\ V_S$ in ft/sec

T = thrust at 100-percent engine speed

D = drag at V_c

REFERENCES

1. Rolls, L. Stewart, and Innis, Robert C.: A Flight Evaluation of a Wing-Shroud-Blowing Boundary-Layer-Control System Applied to the Flaps of an F9F-4 Airplane. NACA RM A55K01, 1956.

2. Cooper, George E., and Innis, Robert C.: Effect of Area-Suction-Type Boundary-Layer Control on the Landing-Approach Characteristics of a 35° Swept-Wing Fighter. NACA RM A55K14, 1956.

3. Anderson, Seth B., and Quigley, Hervey C.: Flight Measurements of the Low-Speed Characteristics of a 35° Swept-Wing Airplane With Area-Suction Boundary-Layer Control on the Flaps. NACA RM A55K29, 1956.

4. Duerfeldt, C. H.: F9F-4 Airplane with Supercirculation Boundary-Layer Control; Performance, Flying Qualities, Landbased and Shipboard Carrier Suitability Evaluation, Letter Rep. No. 1, Final Report. Naval Air Test Center, Patuxent River, Md., Proj. TED No. PTR AD-349, June 2, 1954.

5. Anderson, Seth B., Quigley, Hervey C., and Innis, Robert C.: Flight Measurements of the Low-Speed Characteristics of a 35° Swept-Wing Airplane With Blowing-Type Boundary-Layer Control on the Trailing-Edge Flaps. NACA RM A56G30, 1956.

6. De Leo, Richard V., and Wood, Richard D.: An Experimental Investigation of the Use of Hot Gas Ejectors for Boundary-Layer Control. WADC Tech. Rep. 52-128, Pt. 2, Wright Air Development Center, Dec. 1953.

7. Dannenberg, Robert E., Gambucci, Bruno J., and Weiberg, James A.: Perforated Sheets as a Porous Material for Distributed Suction and Injection. NACA TN 3669, 1956.

8. DeYoung, John: Theoretical Symmetrical Span Loading Due to Flap Deflection for Wings of Arbitrary Plan Form at Subsonic Speeds. NACA Rep. 1071, 1952.

9. Cook, Woodrow L., Holzhauser, Curt A., and Kelley, Mark W.: The Use of Area Suction for the Purpose of Improving Trailing-Edge Flap Effectiveness on a 35° Sweptback Wing. NACA RM A53E06, 1953.

10. Kelley, Mark W., and Tolhurst, William H., Jr.: Full-Scale Wind-Tunnel Tests of a 35° Sweptback Wing Airplane With High Velocity Blowing Over the Trailing-Edge Flaps. NACA RM A55I09, 1955.

11. Perkins, Courtland D., and Hage, Robert E.: Airplane Performance Stability and Control. John Wiley and Sons, Inc., 1949.

12. Dwinnell, James H.: Principles of Aerodynamics. McGraw-Hill Book Co., 1949.

13. Lush, Kenneth J.: Standardization of Take-Off Performance Measurements for Airplanes. TN R-12, AF Flight Test Center, Edwards, Calif., 1954.

TABLE I.- GEOMETRIC DATA FOR TEST AIRPLANE

Wing	
Total area (slatted leading edge), sq ft	288.0
Total area (extended cambered leading edge), sq ft	302.0
Span, ft	37.12
Aspect ratio	4.79
Taper ratio	0.51
Mean aerodynamic chord	8.08
Dihedral angle, deg	3.0
Sweepback of 0.25 chord line, deg	35.2
Geometric twist, deg	2.0
Root airfoil section (normal to 0.25 chord line)	NACA 0012-64 (modified)
Tip airfoil section (normal to 0.25 chord line)	NACA 0011-64 (modified)
Wing area affected by flap, sq ft	116.6
Horizontal tail	
Total area, sq ft	47.2
Span, ft	15.08
Aspect ratio	4.82
Taper ratio	0.45
Sweep, deg	35.0
Vertical tail	
Total area, sq ft	35.1
Span, ft	7.04
Aspect ratio	1.72
Taper ratio	0.37
Sweep, deg	35.0
Flaps	
Total area, sq ft	25.1
Semispan, ft	7.46
Chord, ft	1.71

TABLE II.- STALLING AND APPROACH CHARACTERISTICS

(a) Cambered leading edge

Pilot	BLC	Stall			Field carrier-landing approach (gross weight 13,850 lb)	
		Speed, knots	Gross weight, lb	Characteristics	Speed, knots	Reason for limiting approach speed
A	Blowing (0.02 in. nozzle)	92.0	13,850	Unsatisfactory roll-off with inadequate buffet warning	101.5	Proximity to stall
	Blowing (0.01 in. nozzle)	92.0	13,850		101.5	
	Suction	95.0	13,850		109.0	Ability to stop rate of sink
	Off	98.5	13,850	Unsatisfactory roll-off with inadequate buffet warning (roll-off less abrupt)	109.0	Proximity to stall
B	Blowing (0.02 in. nozzle)	92.0	13,850	Stall marginal due to roll-off with no stall warning	101.5	Proximity to stall
	Blowing (0.01 in. nozzle)	93.0	13,850		104.5	
	Suction	98.5	15,260		107.0	
	Off	97.0	14,470	Stall marginal due to roll-off with inadequate warning	112.0	Proximity to stall and ability to control altitude
D	Blowing (0.02 in. nozzle)	94.0	15,190	Unsatisfactory roll-off with inadequate buffet warning	102.5	Proximity to stall
	Blowing (0.01 in. nozzle)	91.0	13,850		104.5	
	Suction	99.5	15,150		107.0	
	Off	100.0	15,350	Unsatisfactory roll-off with inadequate buffet warning (roll-off more abrupt)	112.0	

TABLE II.- STALLING AND APPROACH CHARACTERISTICS - Concluded
(b) Slatted leading edge

Pilot	Flap configuration	BLC	Stall			Field carrier-landing approaches		
			Speed, knots	Gross weight, lb	Characteristics	Speed, knots	Gross weight, lb	Reason for limiting approach speed
A	55°	Off	101	15,250	Buffet and lateral instability at 103 knots	108	13,850	Proximity to stall
	55°	Suction	99	15,150	Buffet and lateral instability at 101 knots	108	13,850	
	55°	Blowing (0.01 in. nozzle)	92	13,850	Warning: marginal Stall: satisfactory	104	13,850	Inadequate altitude control
	45° slotted	None	96	13,680		108-113	13,680	
B	55°	Off	101	14,850	Buffet at 103 knots	110	13,850	Ability to control altitude
	55°	Suction	100	14,850	Buffet and pitch-up at 101 knots	105.5	13,850	Proximity to stall
	55°	Blowing (0.01 in. nozzle)	---	---	---	102.5	13,850	Inadequate altitude control
	45° slotted	None	96	13,680	Warning: marginal Stall: satisfactory	113	13,680	
C	55°	Off	100	14,350	Slight pitch-up and rolling tendency to right	108	13,850	Proximity to stall
	55°	Suction	99	14,380	Slight pitch-up and rolling tendency to right preceded by buffet	104-108	13,850	
D	55°	Off	---	---	---	112	13,850	Inadequate altitude control
	55°	Blowing (0.01 in. nozzle)	---	---	---	101.5	13,850	
	45° slotted	None	96	13,680	Warning: marginal Stall: satisfactory	113	13,680	

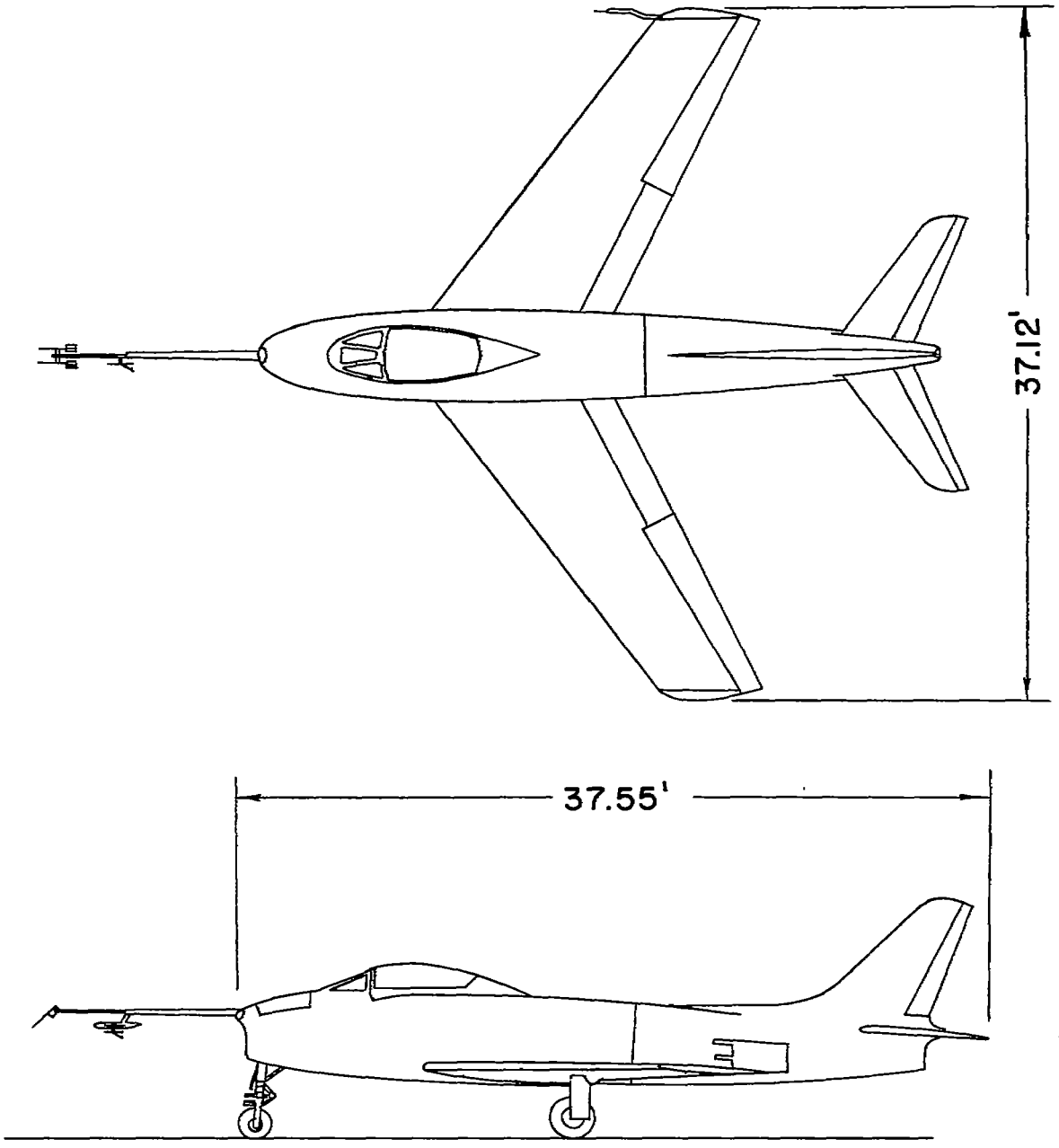

Figure 1.- Two-view drawing of test airplane.

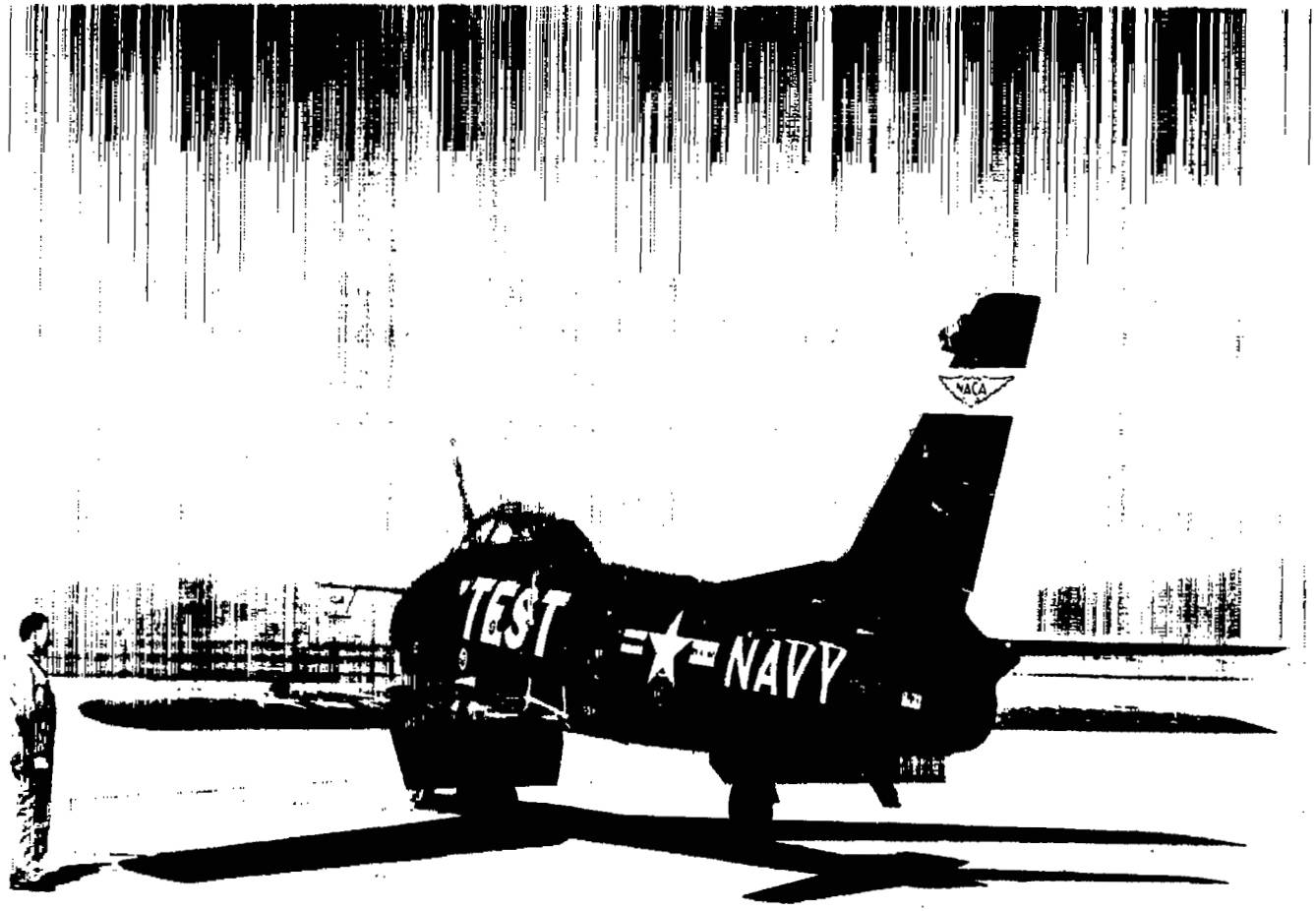

Figure 2.- Photograph of test airplane.

A-21284

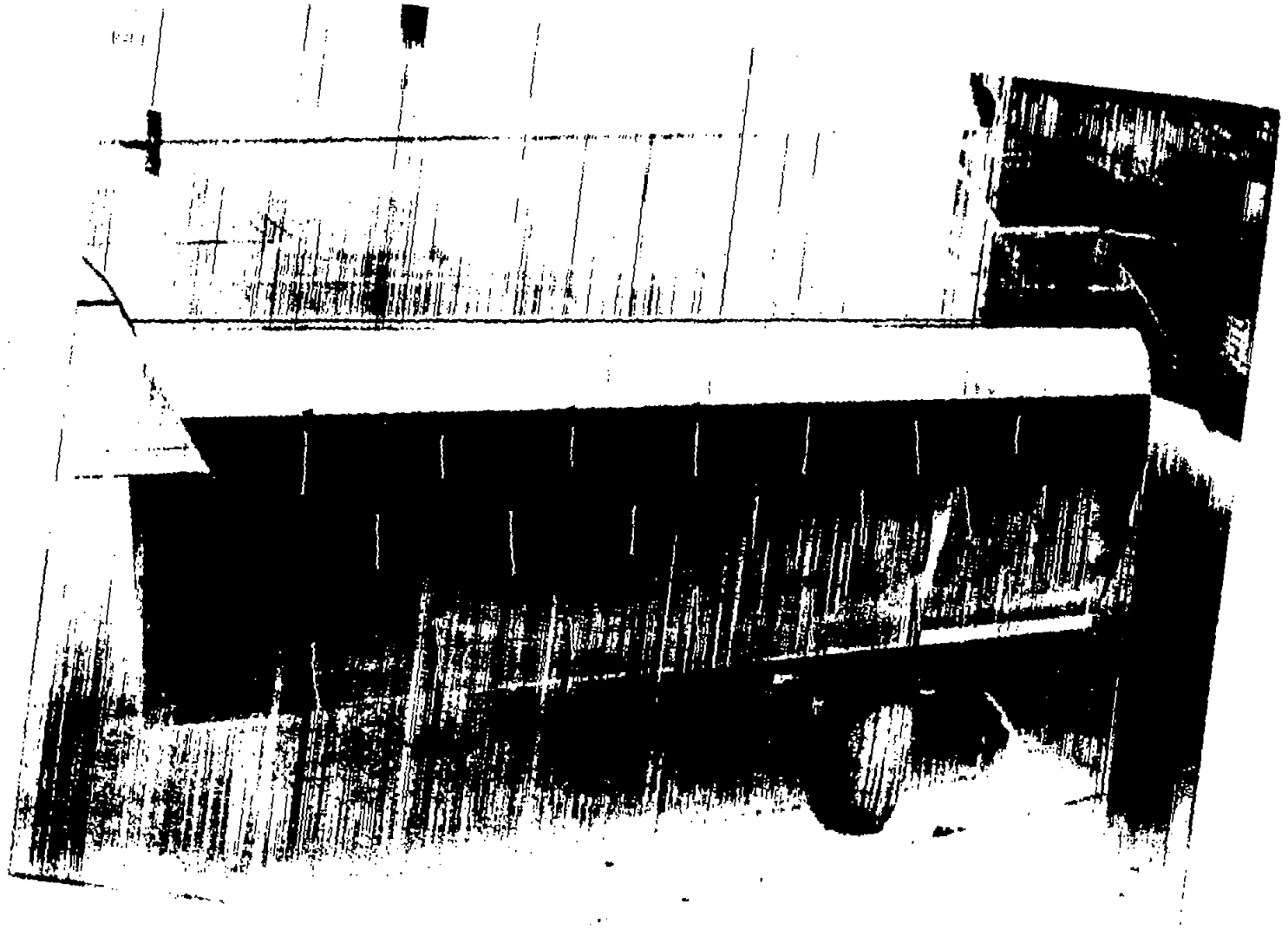

Figure 3.- Photograph of area-suction boundary-layer control flap. A-20816

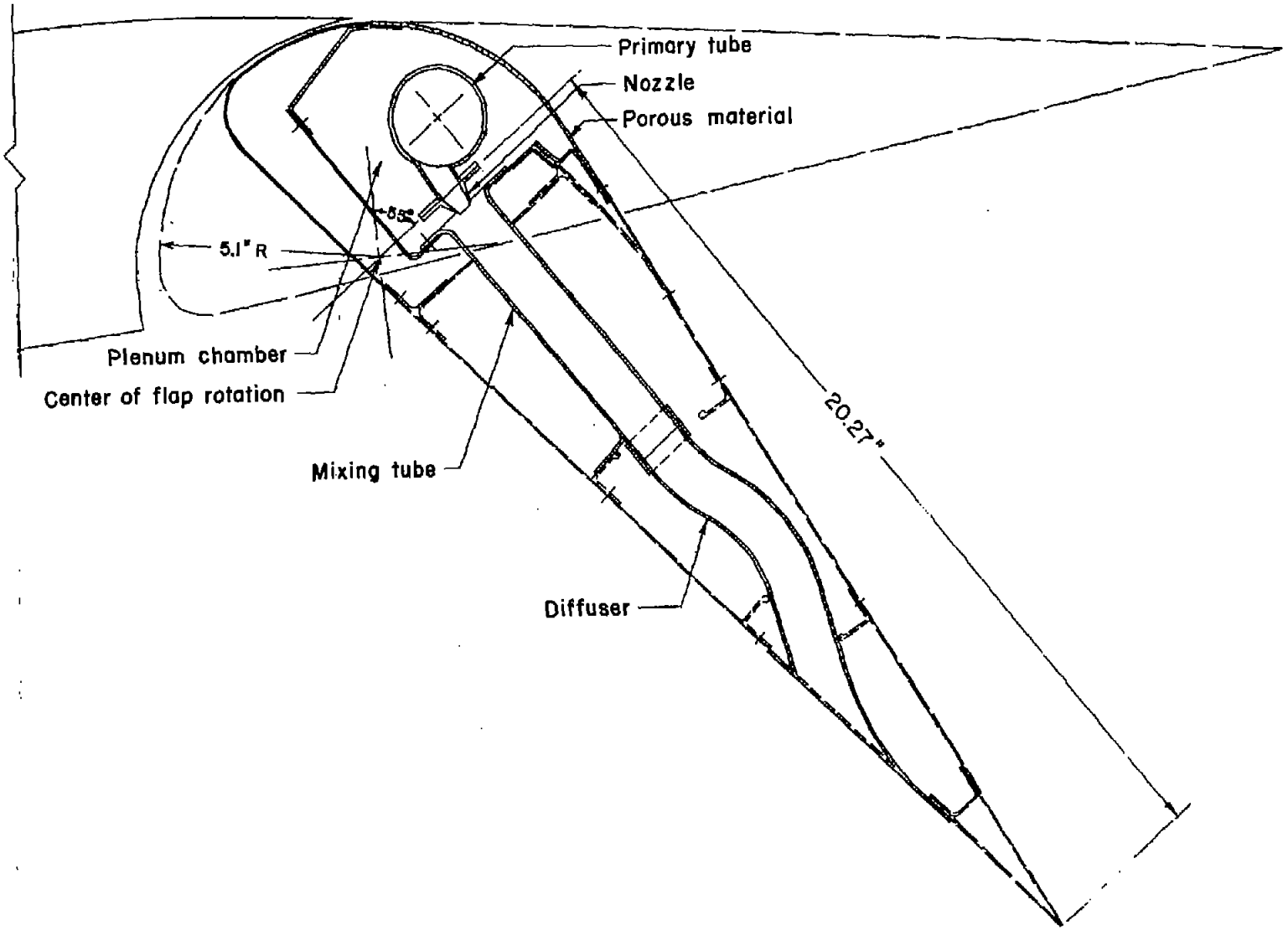

Figure 4.- Typical cross section of suction flap.

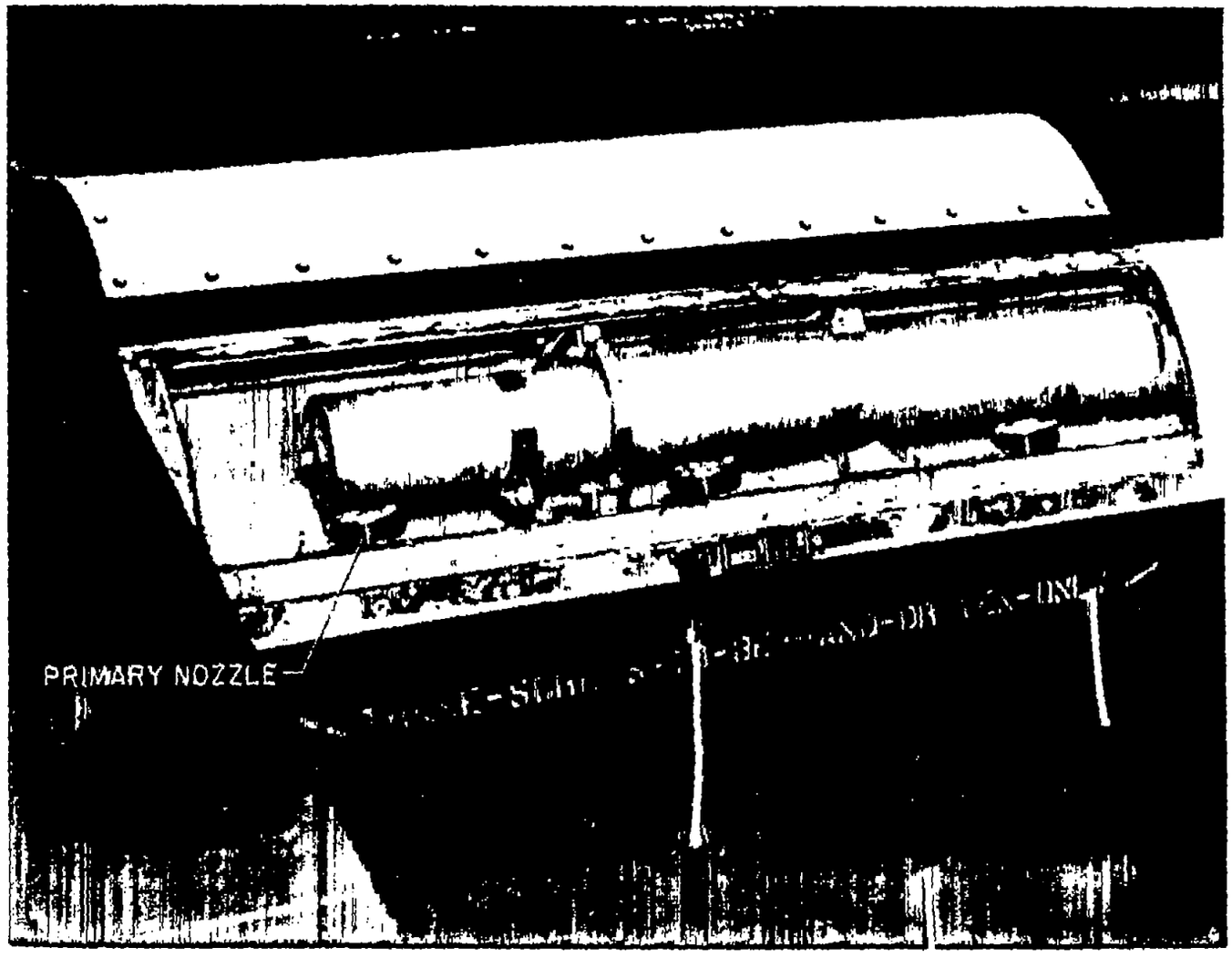

(a) Flap with a portion of sintered porous material removed.

A-20517.1

Figure 5.- Close-up of area-suction flap.

A-21112

(b) Ejector pump exits.

Figure 5.- Concluded.

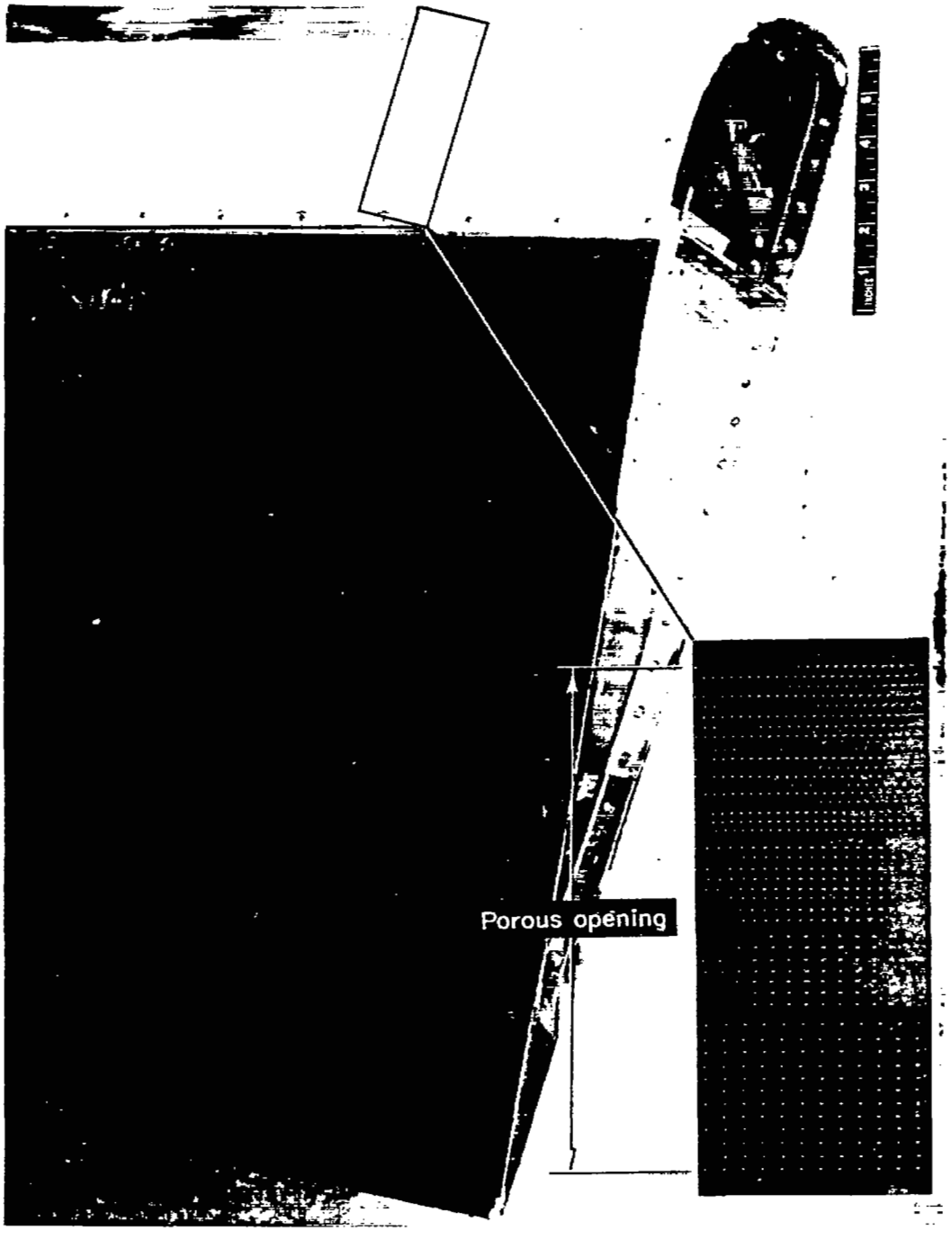

A-21219.2

Figure 6.- Close-up of area-suction flap with perforated porous material.

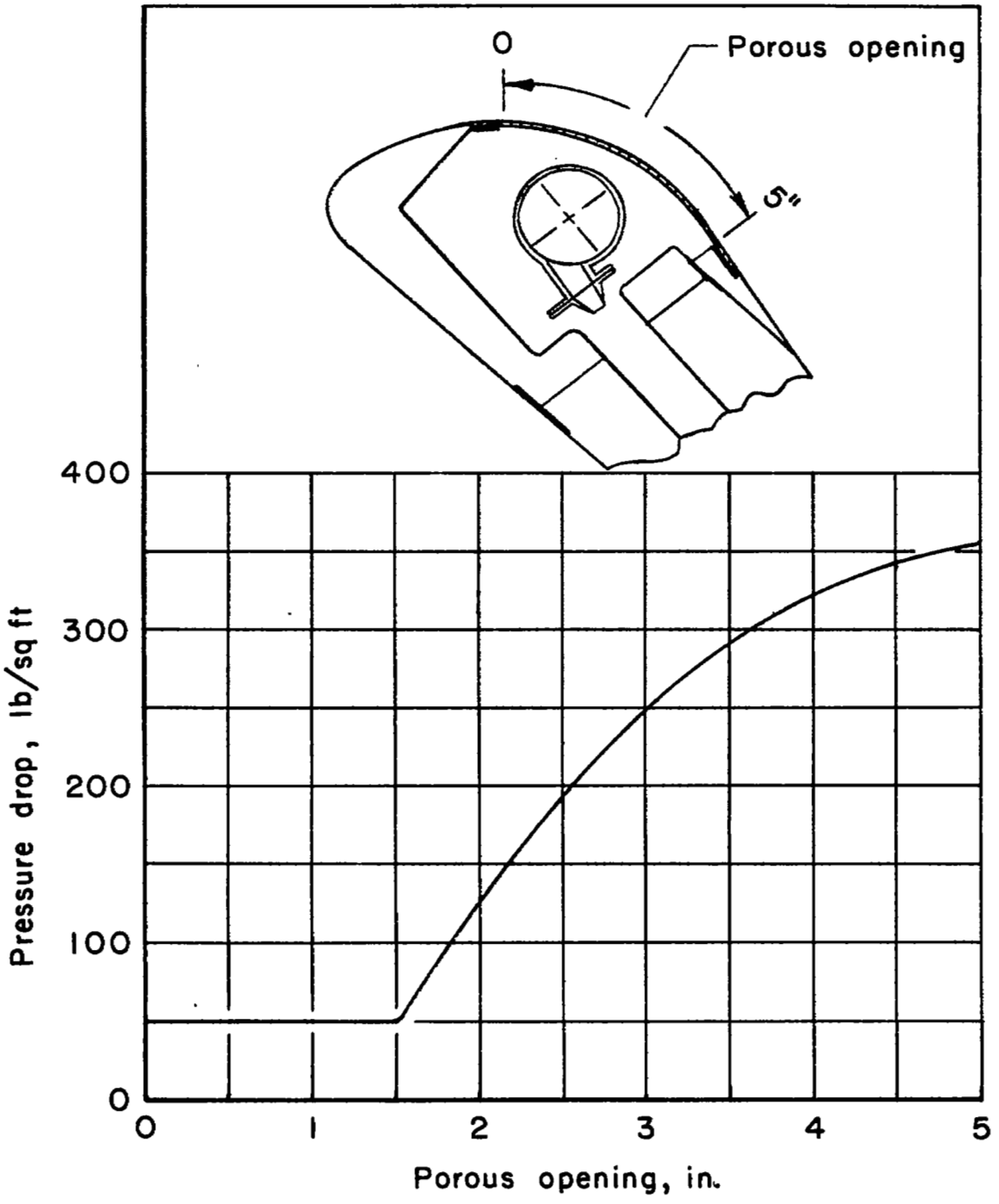

Figure 7.- Design variation of pressure drop across porous material with chordwise opening; inflow velocity 4.4 ft/sec.

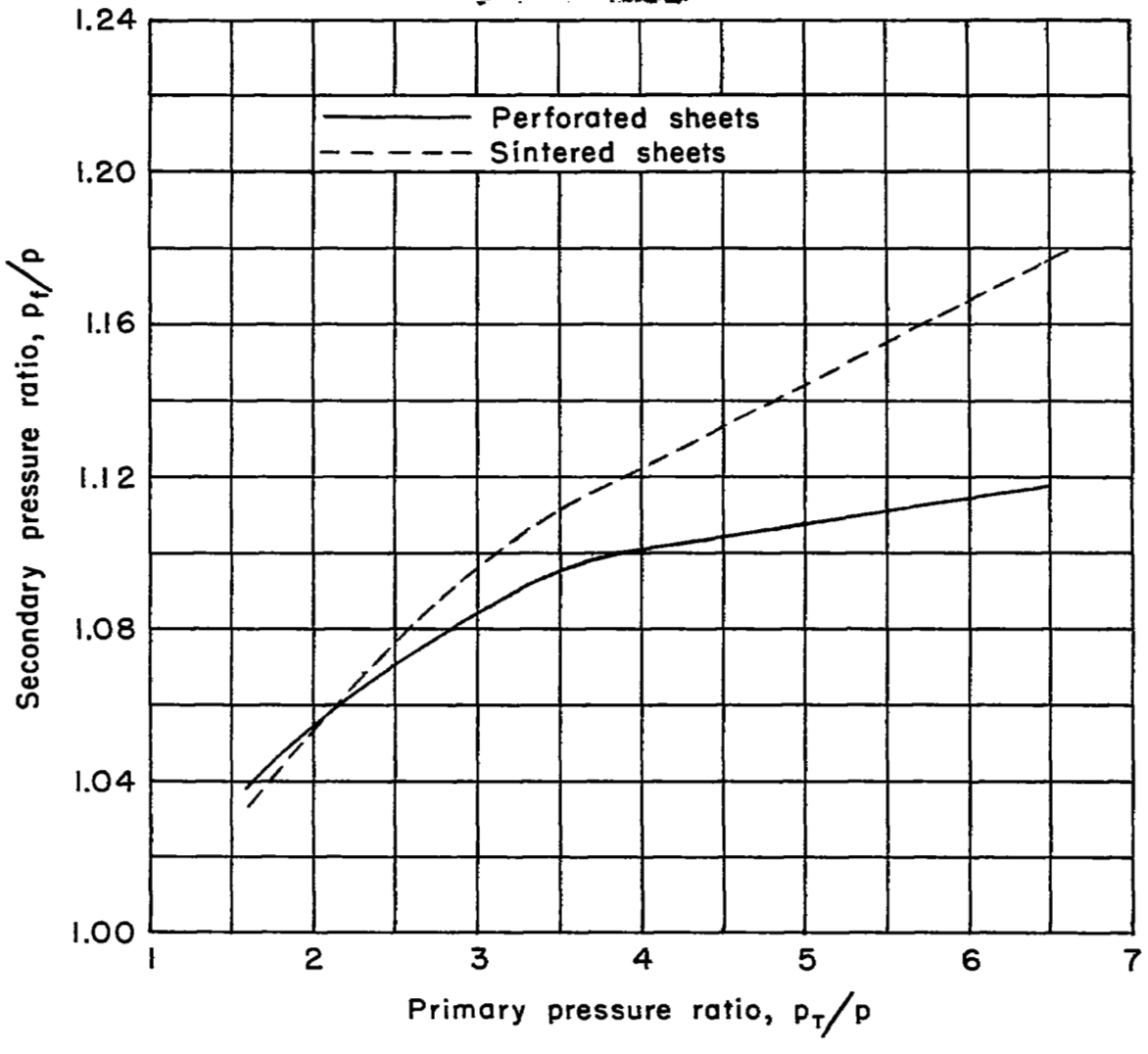

Figure 8.- Ejector pump characteristics with two types of porous materials.

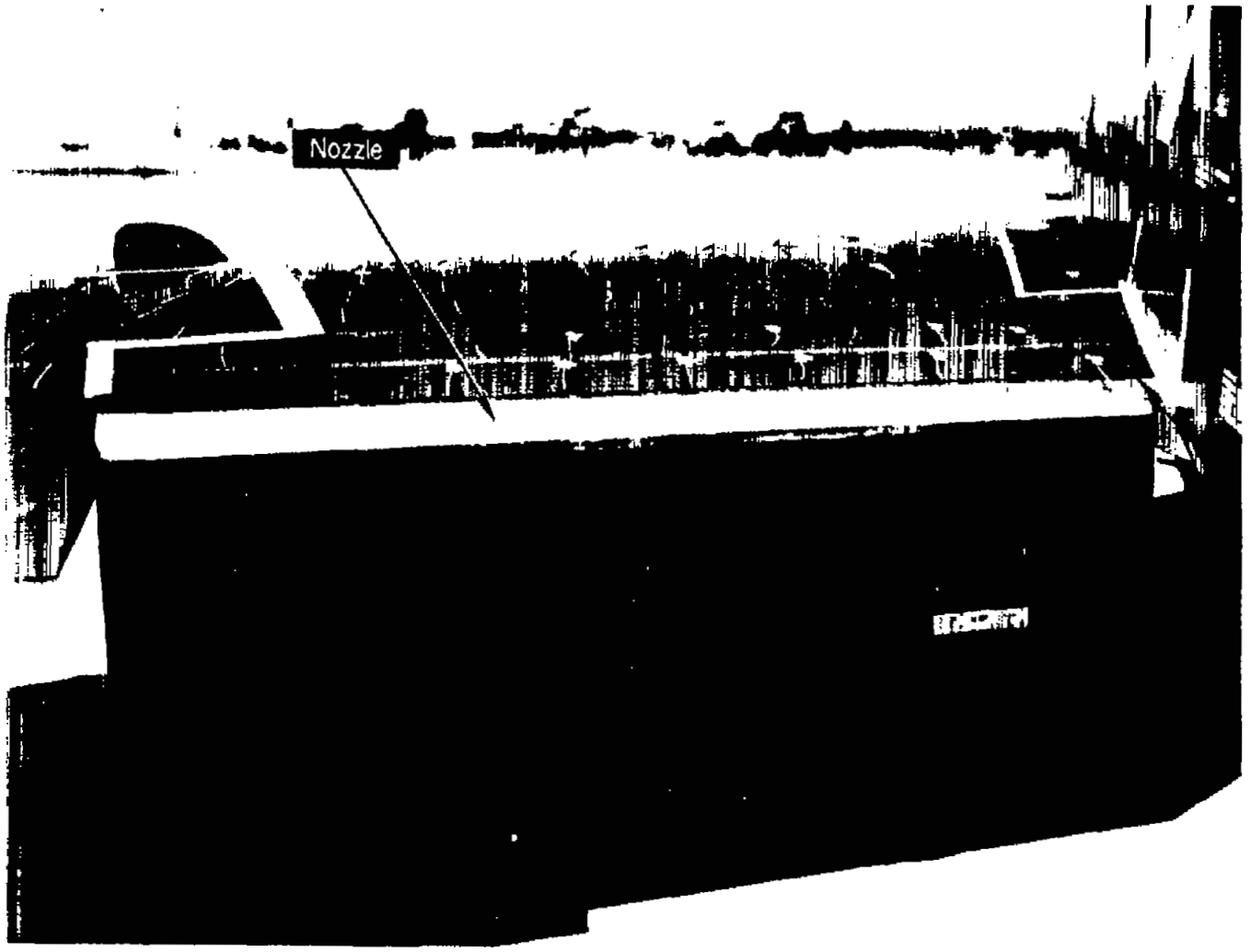

A-21285.1

Figure 9.- Photograph of blowing boundary-layer control flap.

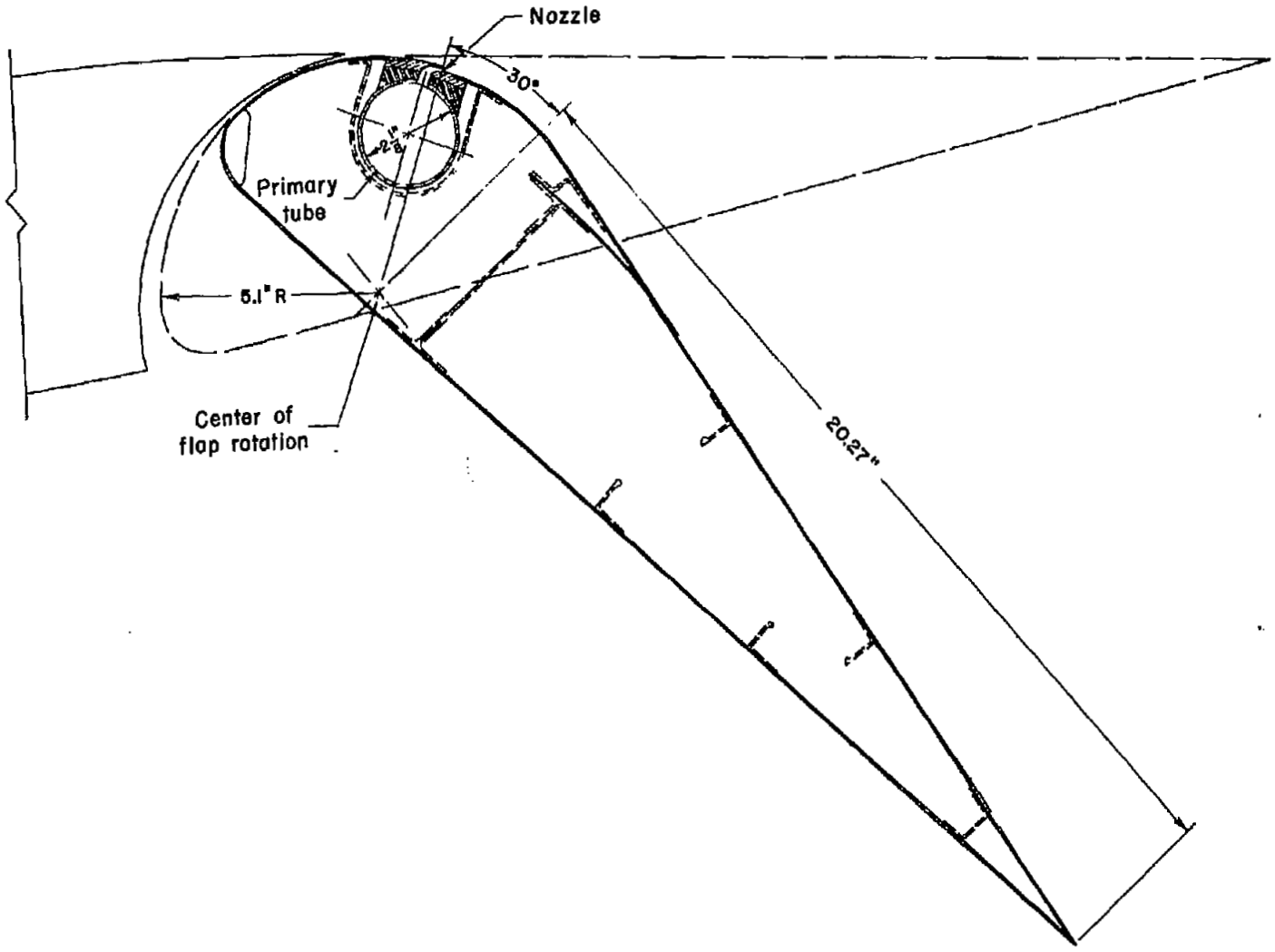

Figure 10.- Typical cross section of the blowing flap.

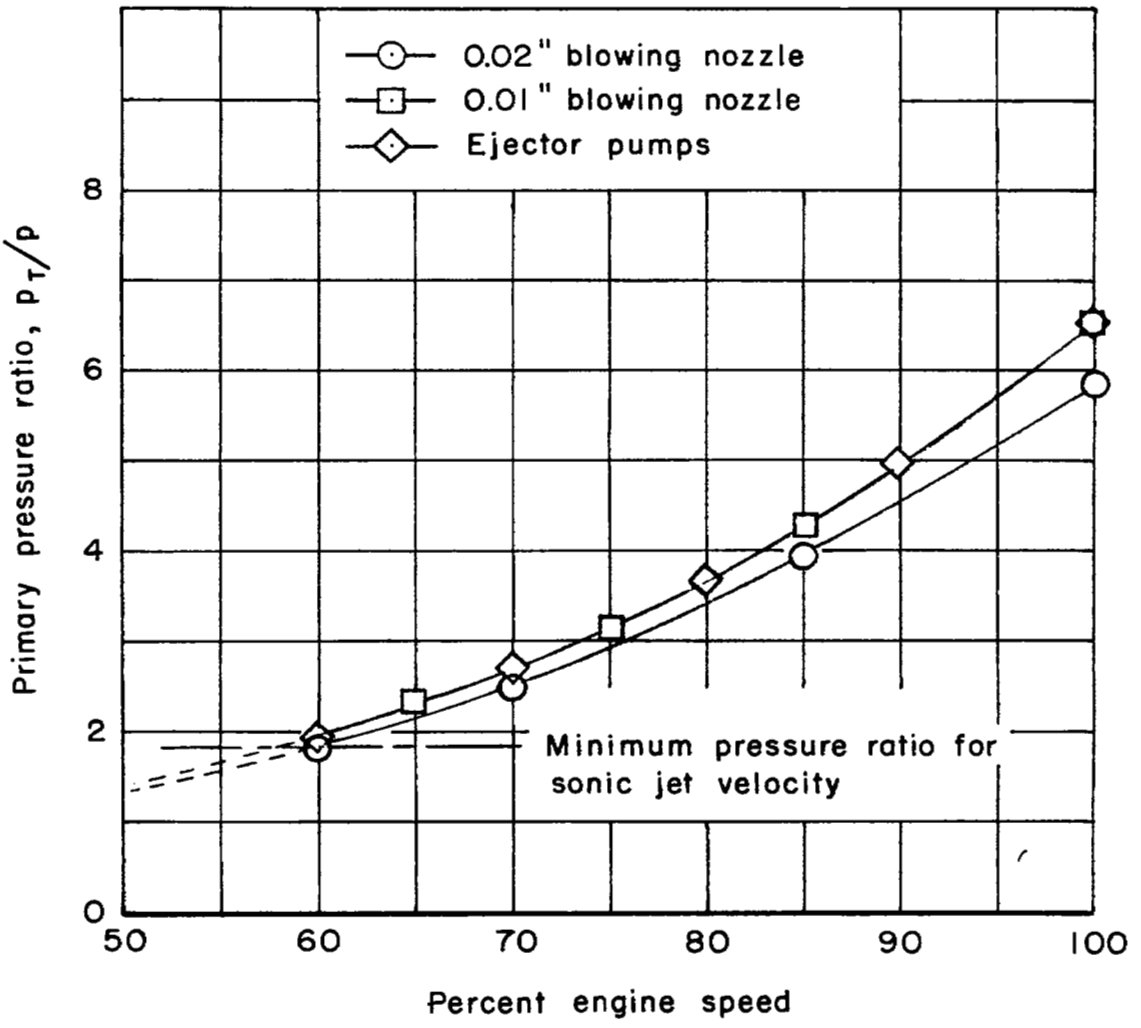

Figure 11.- Variation of engine bleed-air pressure ratio with engine speed.

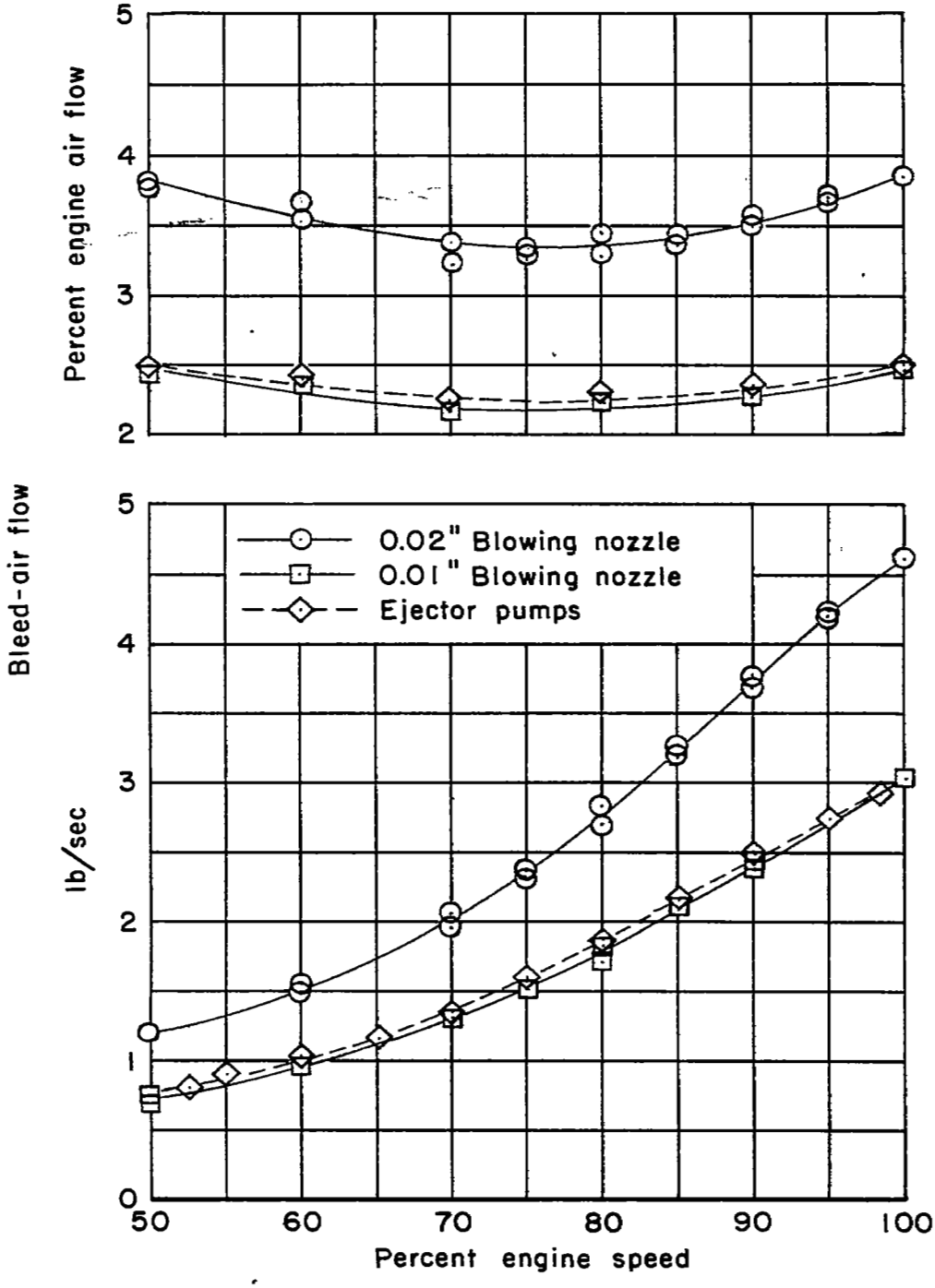

Figure 12.- Variation of bleed-air flow with engine speed.

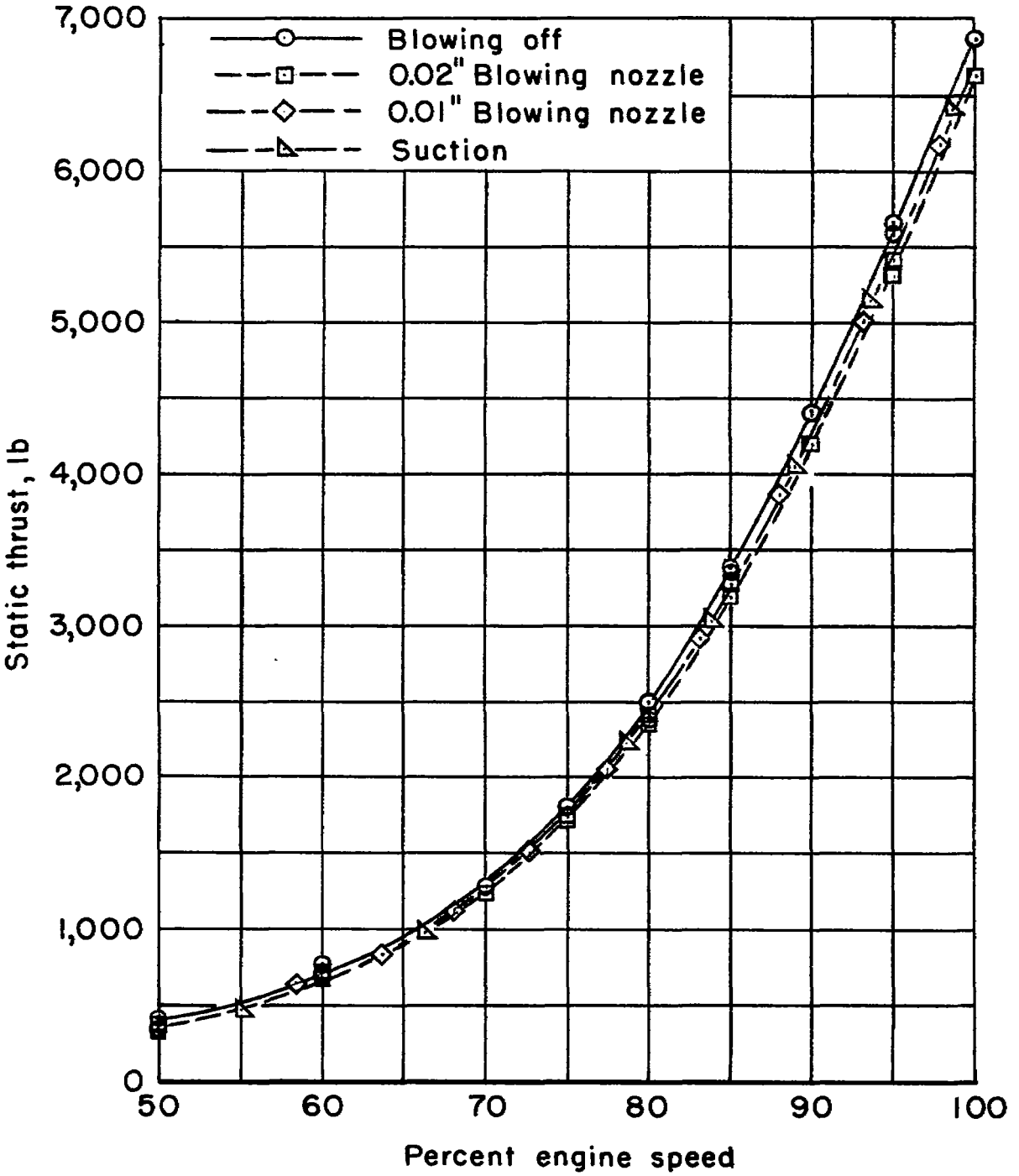

Figure 13.- Variation of static thrust with engine speed.

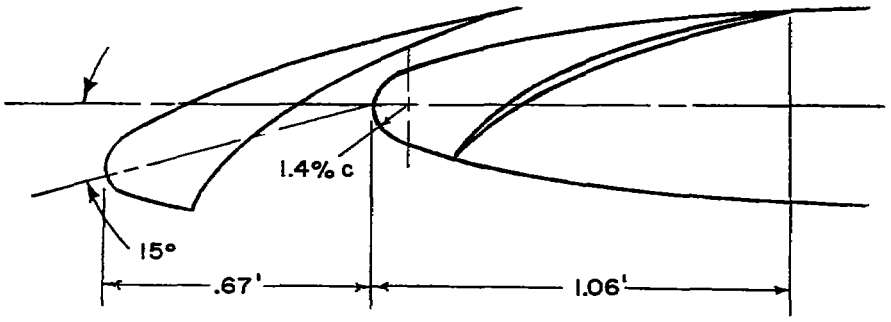

Slat extended and retracted - Wing station .857 b/2.
Slat extent; .24 b/2 to .96 b/2.

(a) Slatted leading edge.

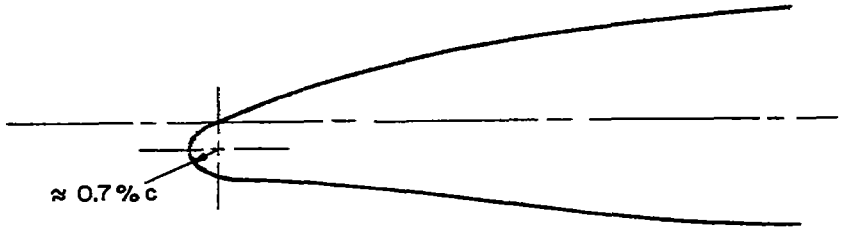

NACA 23009 cambered section — Wing station .857 b/2.
Cambered section full span.

(b) Extended cambered leading edge.

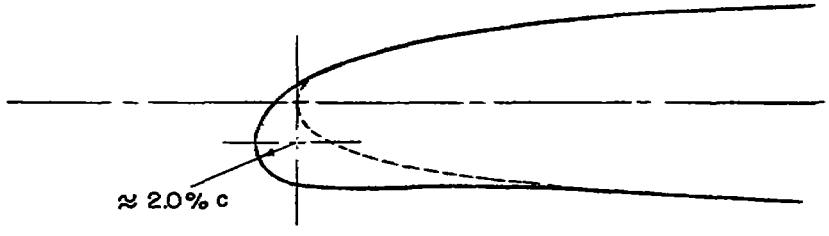

NACA 23012 cambered section - Wing station .22 b/2.
Extent of camber; .08 b/2 to .22 b/2.

(c) Modified inboard section of slatted leading edge.

Figure 14.- Cross section of various leading-edge configurations.

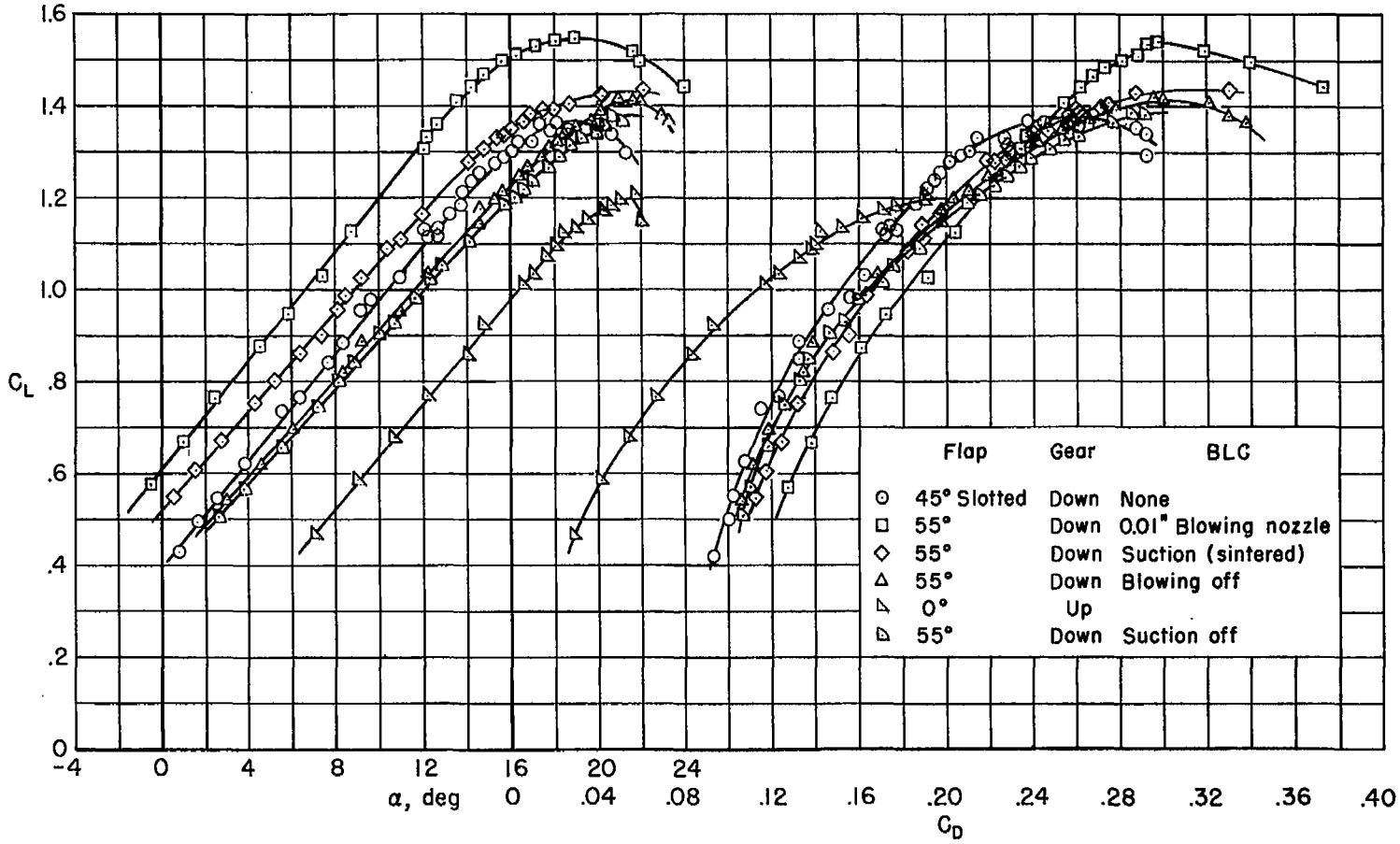

(a) Slatted leading edge.

Figure 15.- Lift and drag characteristics for various configuration; 85-percent engine speed.

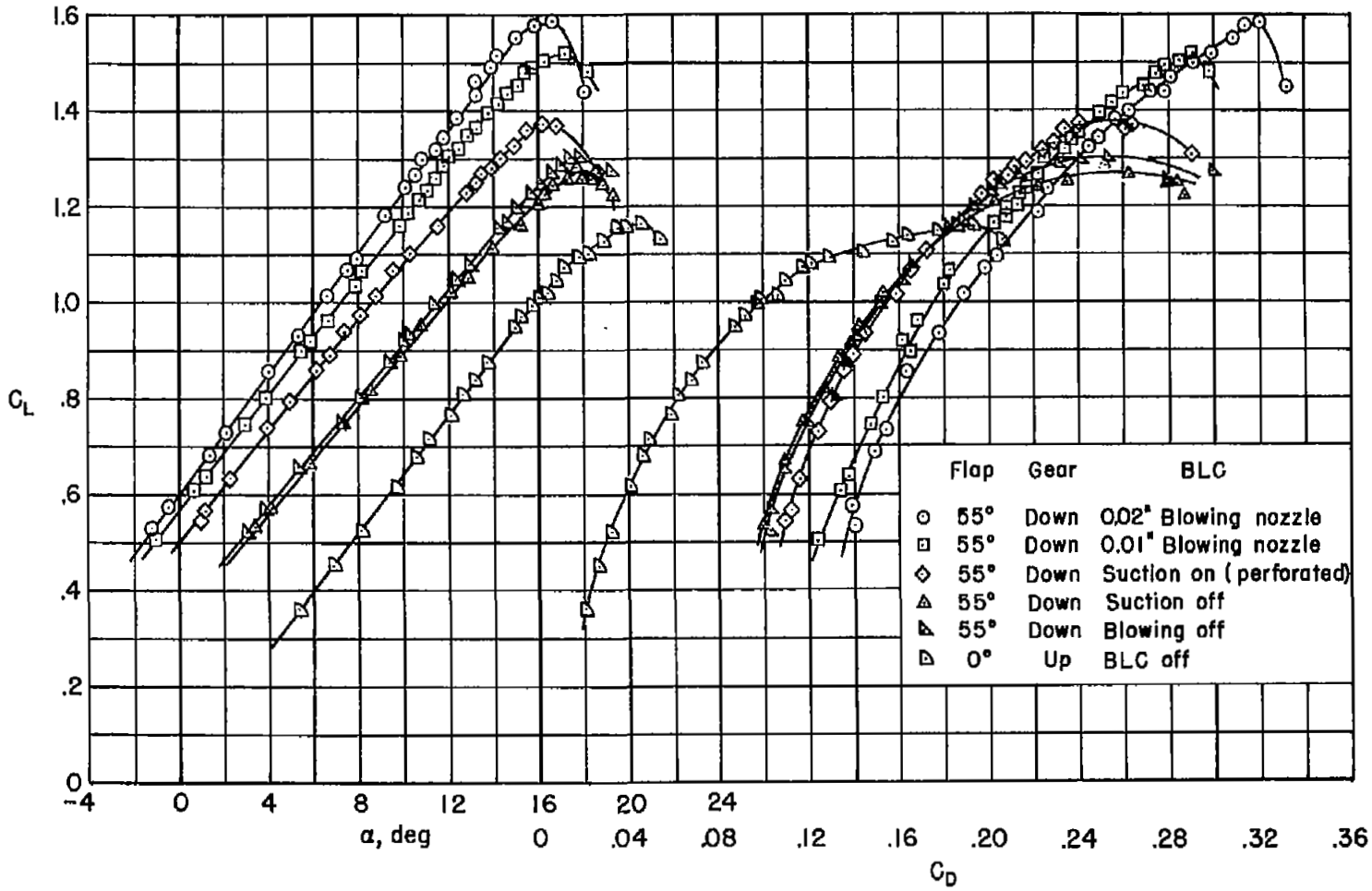

(b) Extended cambered leading edge.

Figure 15.- Concluded.

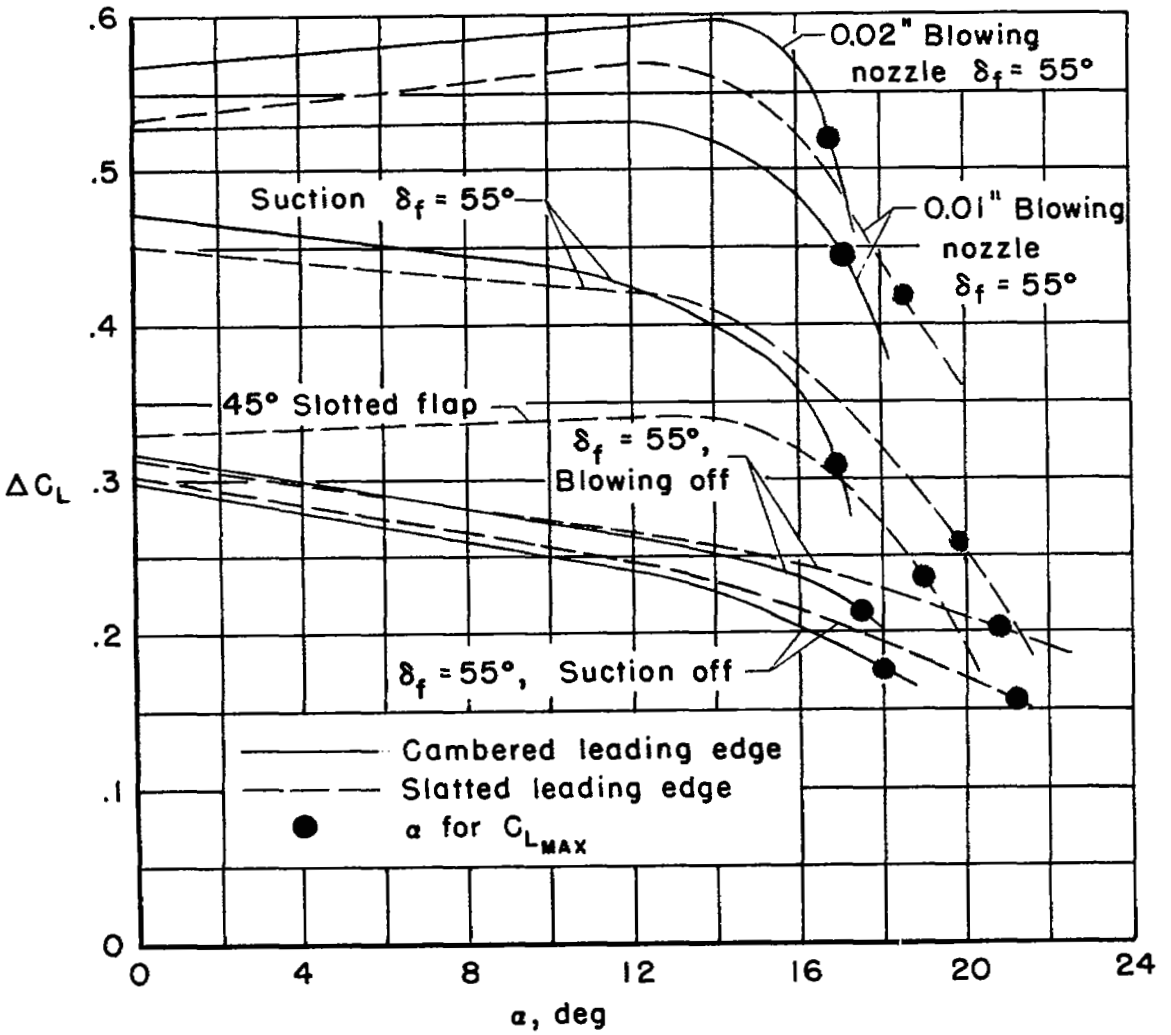

Figure 16.- Variation of flap lift with angle of attack; 85-percent engine speed.

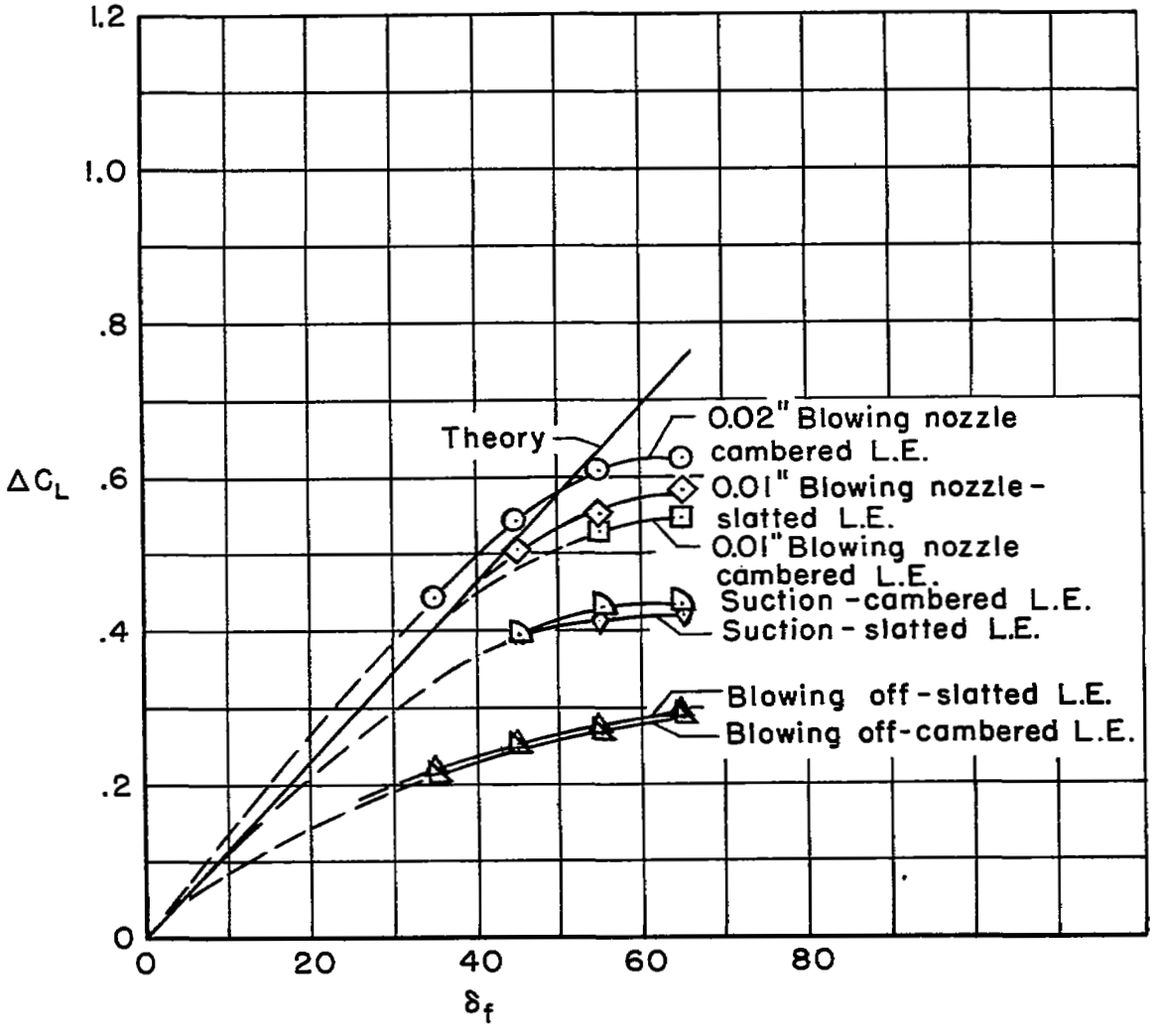

Figure 17.- Variation of flap lift increment with flap deflection; $\alpha=12^{\circ}$, 85-percent engine speed.

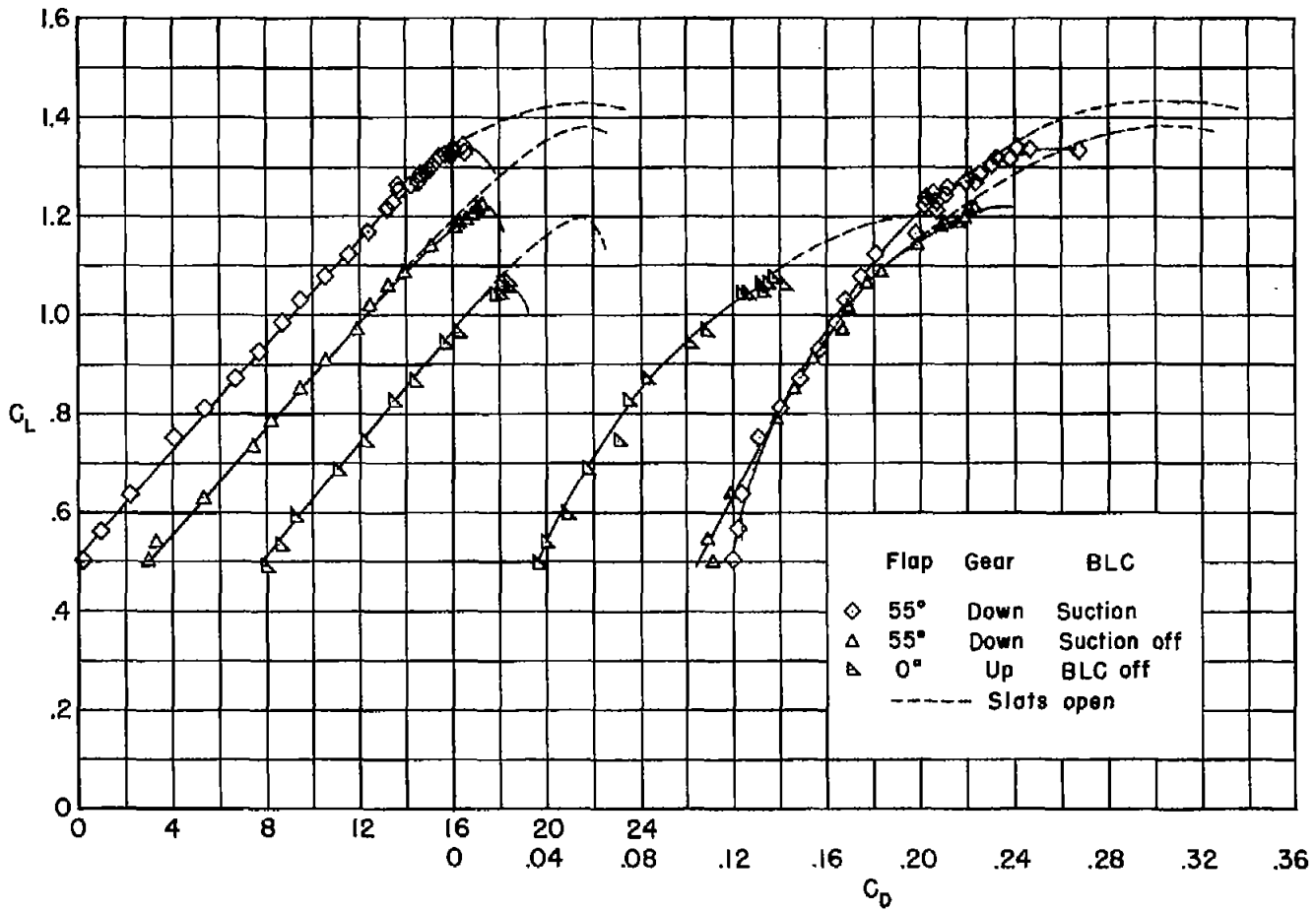

(a) Slats locked closed and sealed.

Figure 18.- Lift and drag characteristics for various leading-edge configurations; 85-percent engine speed.

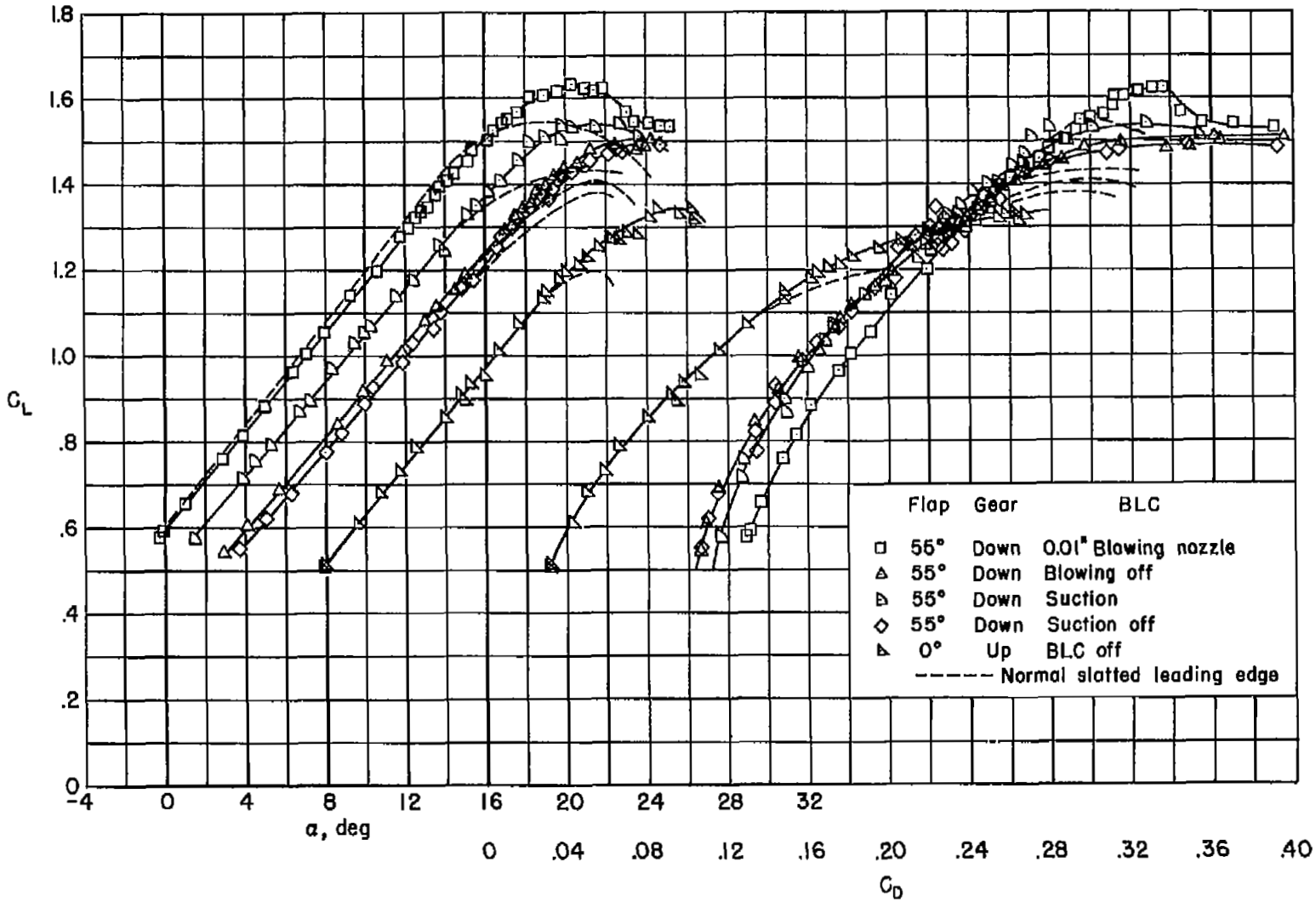

(b) Slatted leading edge with modified inboard section.

Figure 18.- Continued.

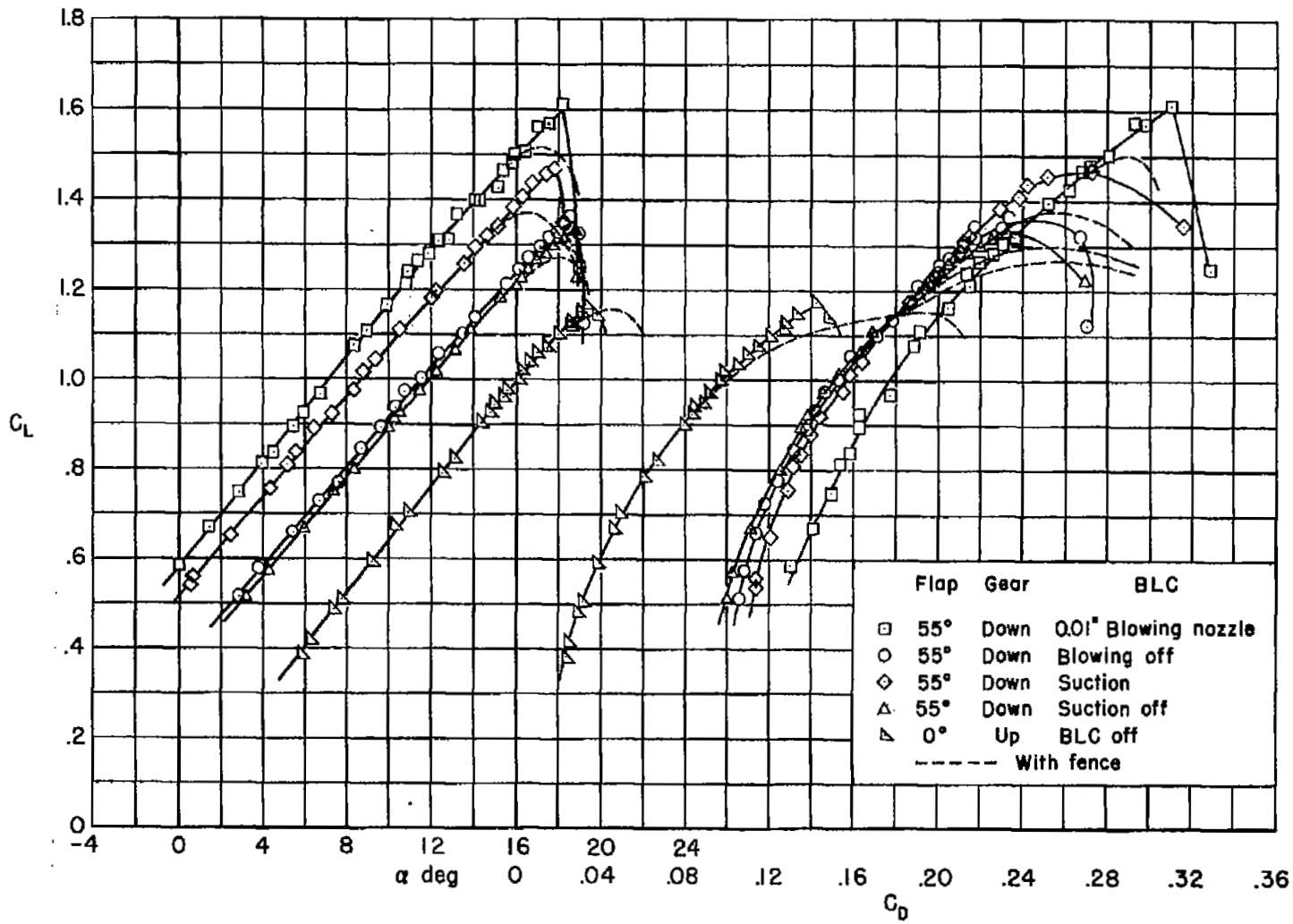

(c) Cambered leading edge without fence.

Figure 18.- Concluded.

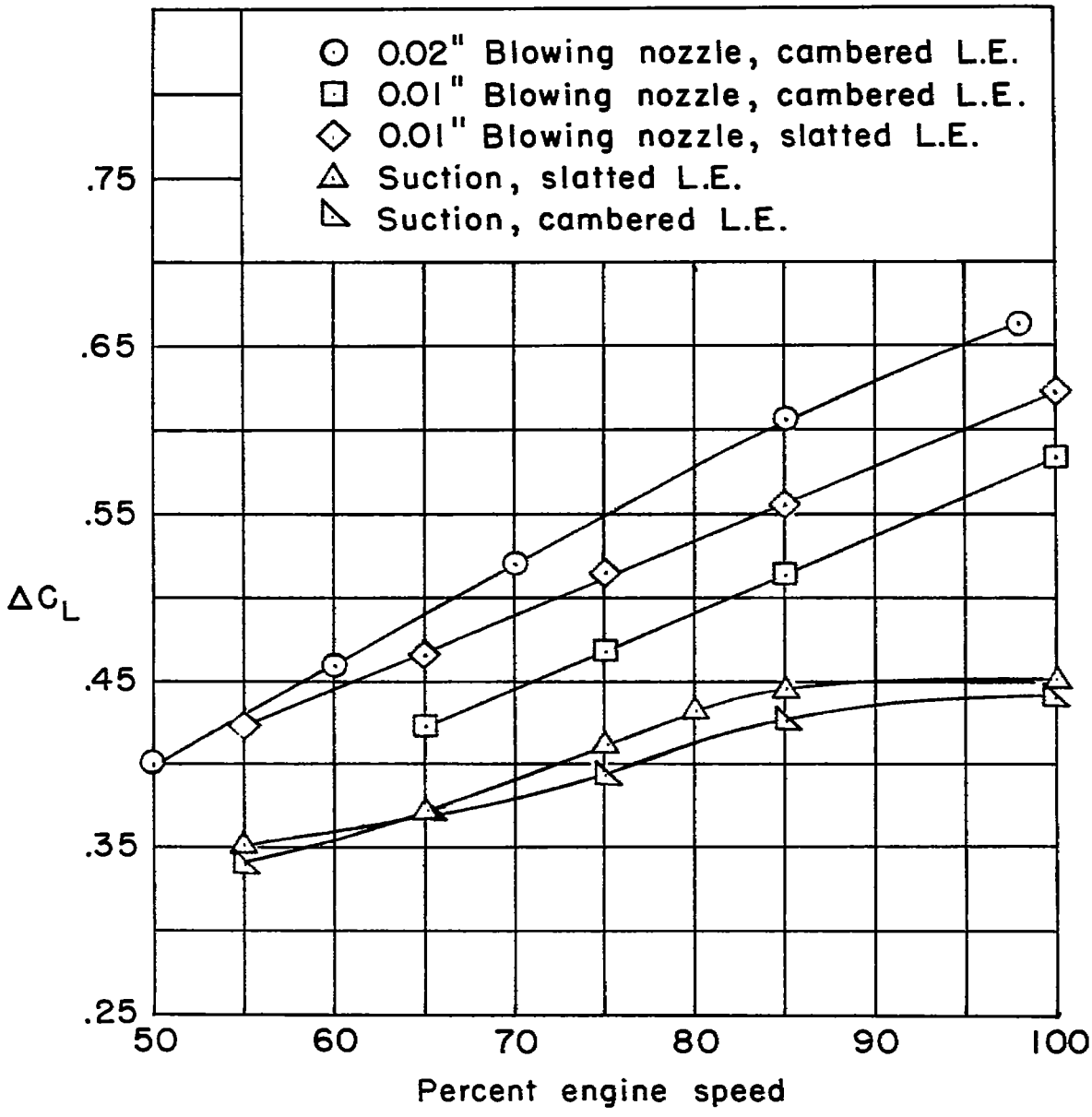

Figure 19.- Variation of flap lift increment with engine speed; $\delta_f = 55^\circ$, $\alpha = 12^\circ$.

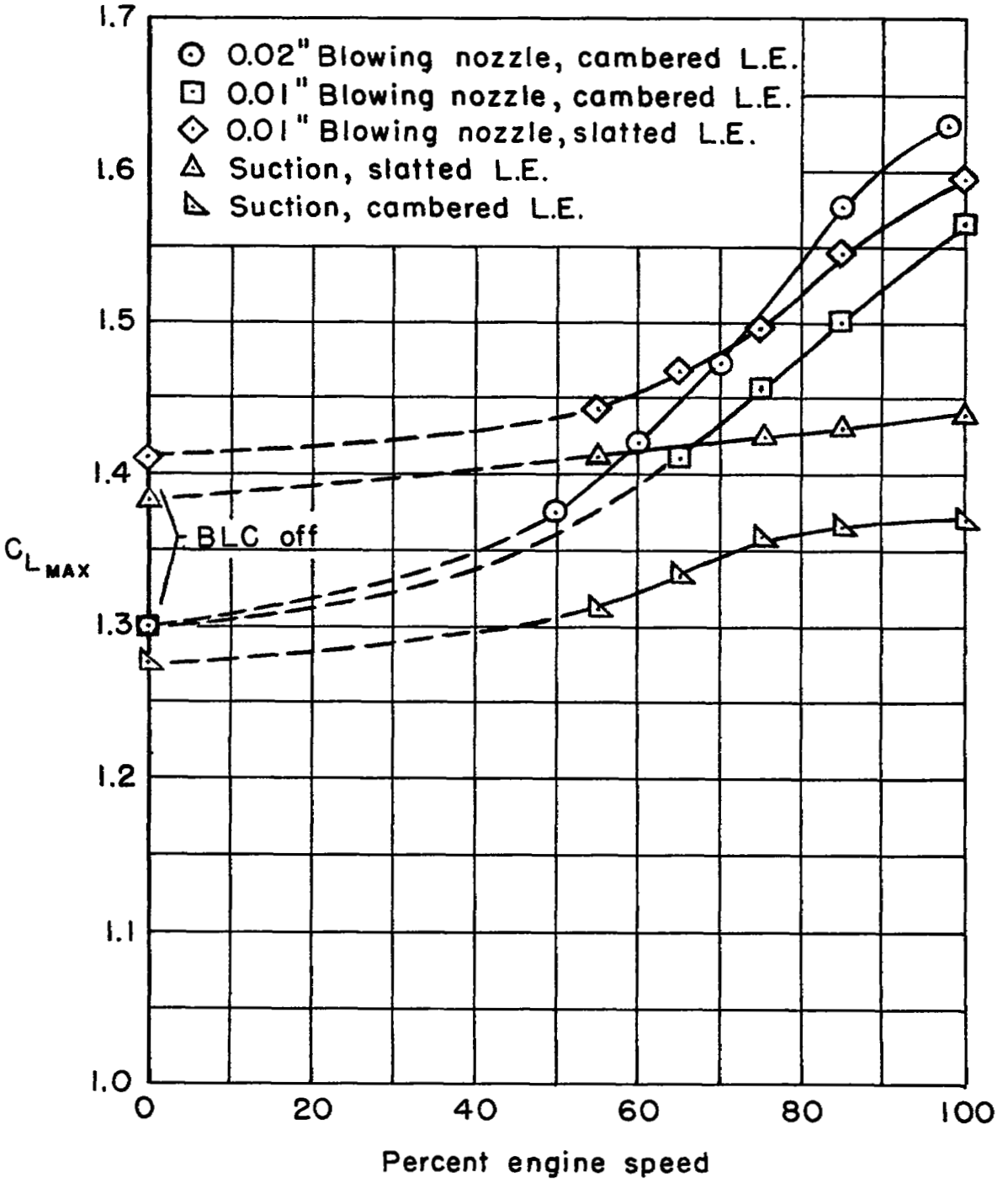

Figure 20.- Variation of maximum lift coefficient with engine speed; $\delta_f = 55^\circ$.

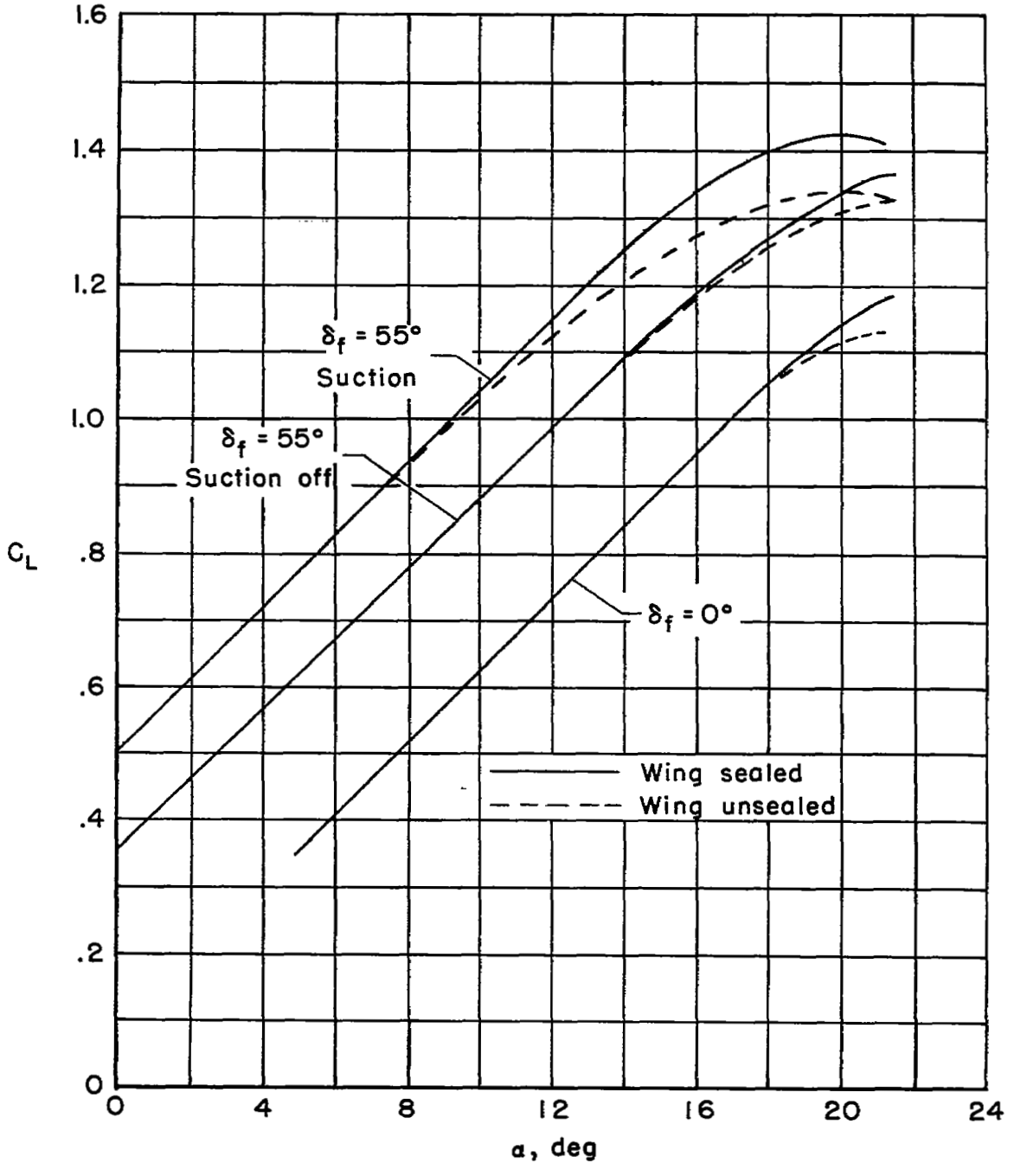

Figure 21.- Lift curves for wing sealed and unsealed; gear down, slatted leading edge.

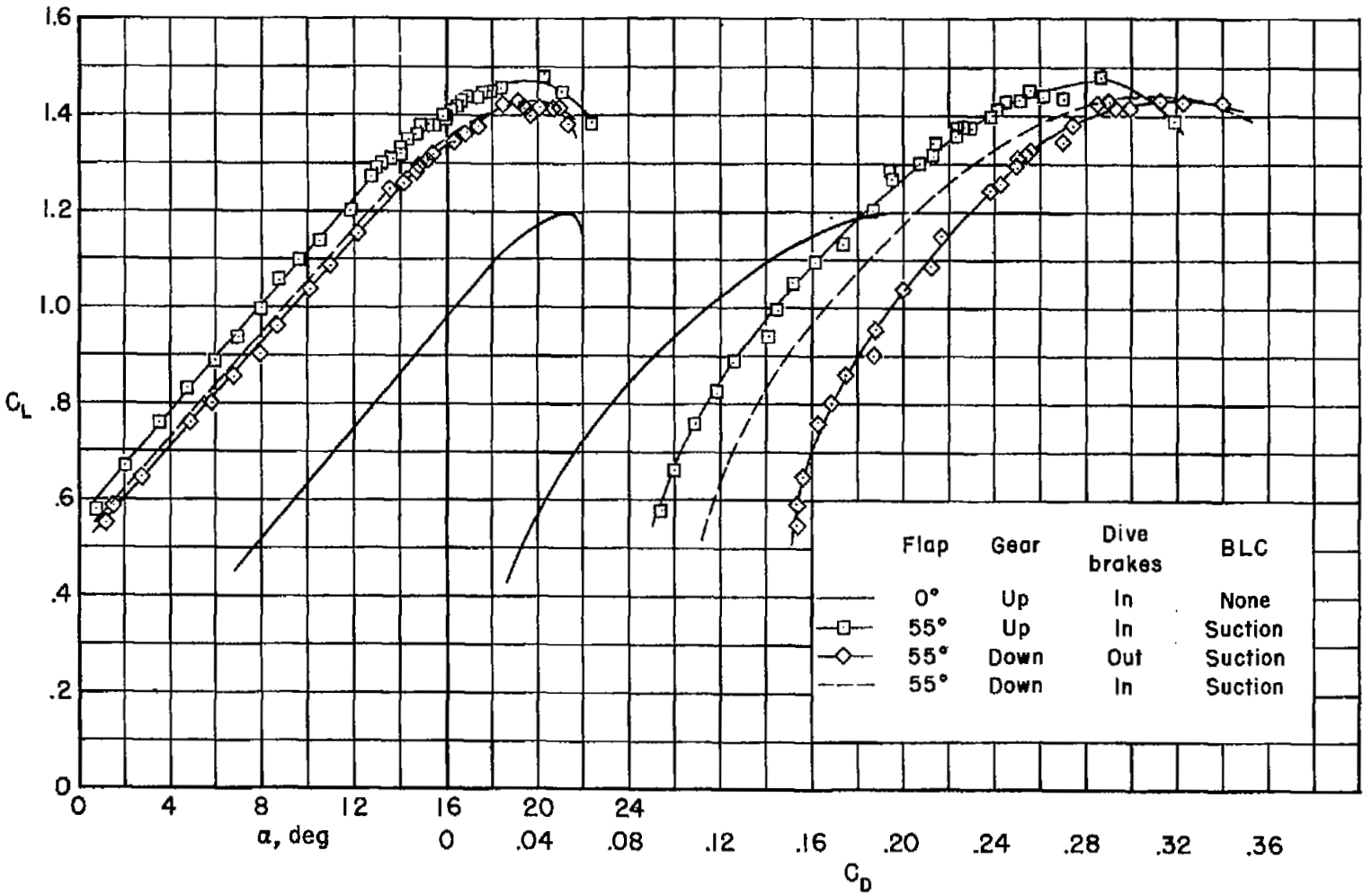

Figure 22.- Effect of landing gear and dive brakes on lift and drag; slatted leading edge.

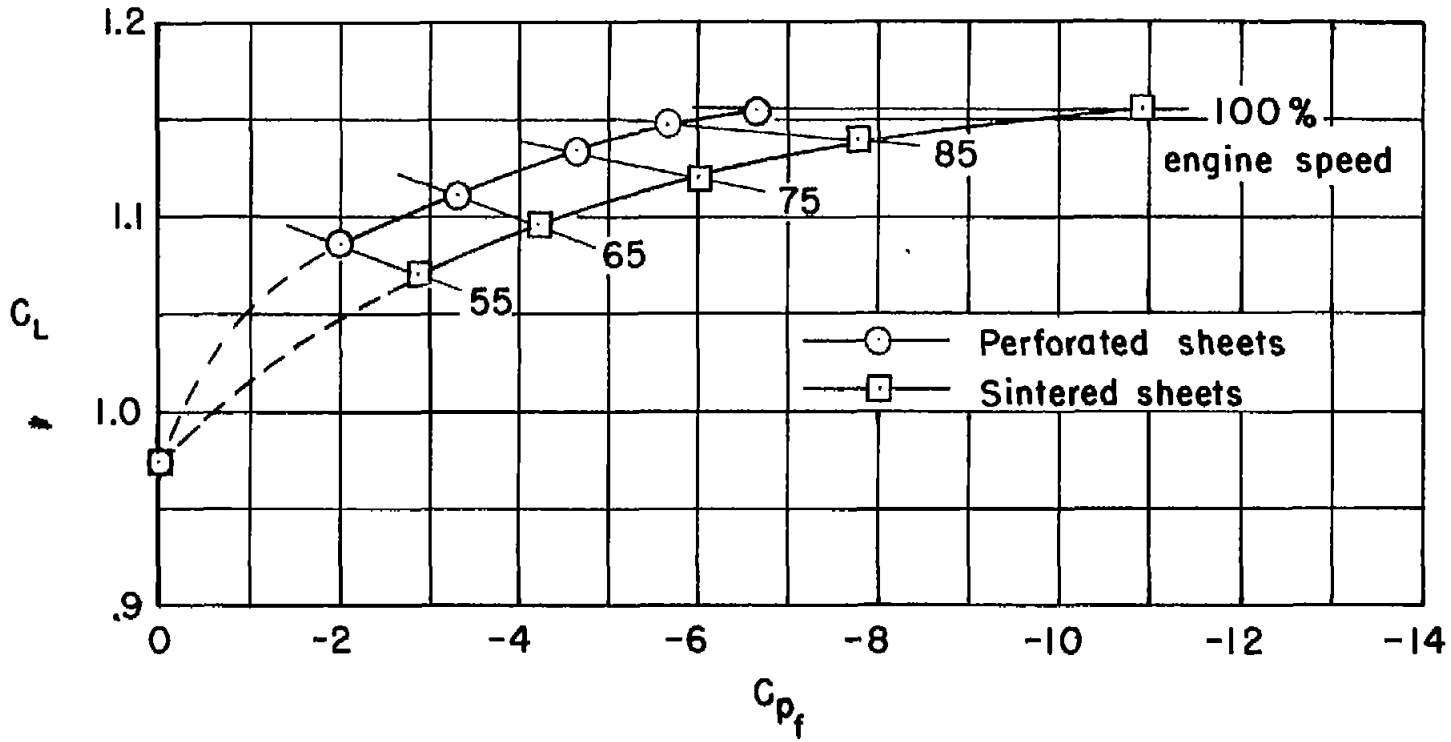

Figure 23.- Variation of lift coefficient with flap plenum-chamber pressure coefficient; $\delta_f = 55^\circ$, $\alpha = 12^\circ$.

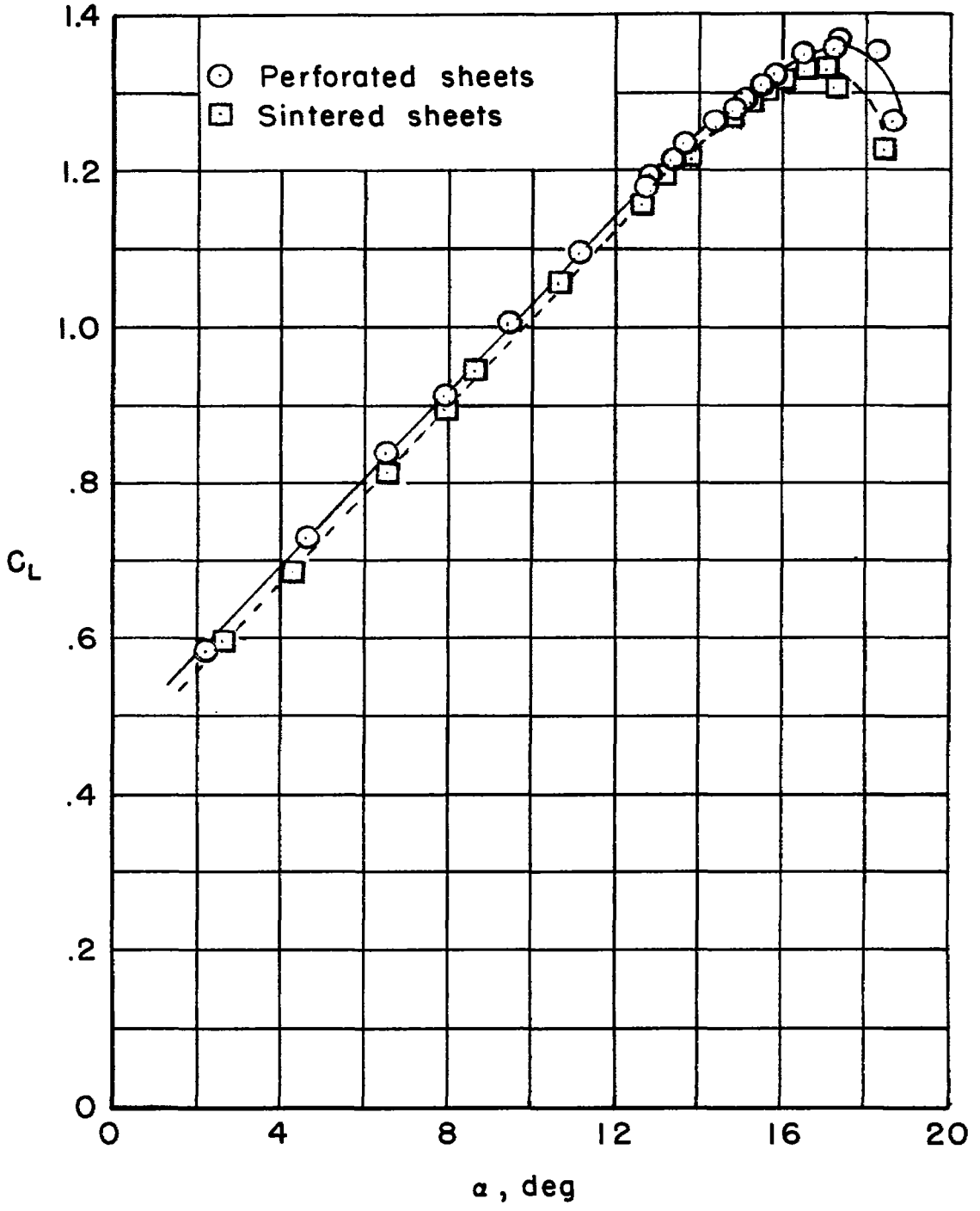

Figure 24.- Lift curves for suction flap with perforated and sintered porous materials; $\delta_f = 55^\circ$, 85-percent engine speed, gear down.

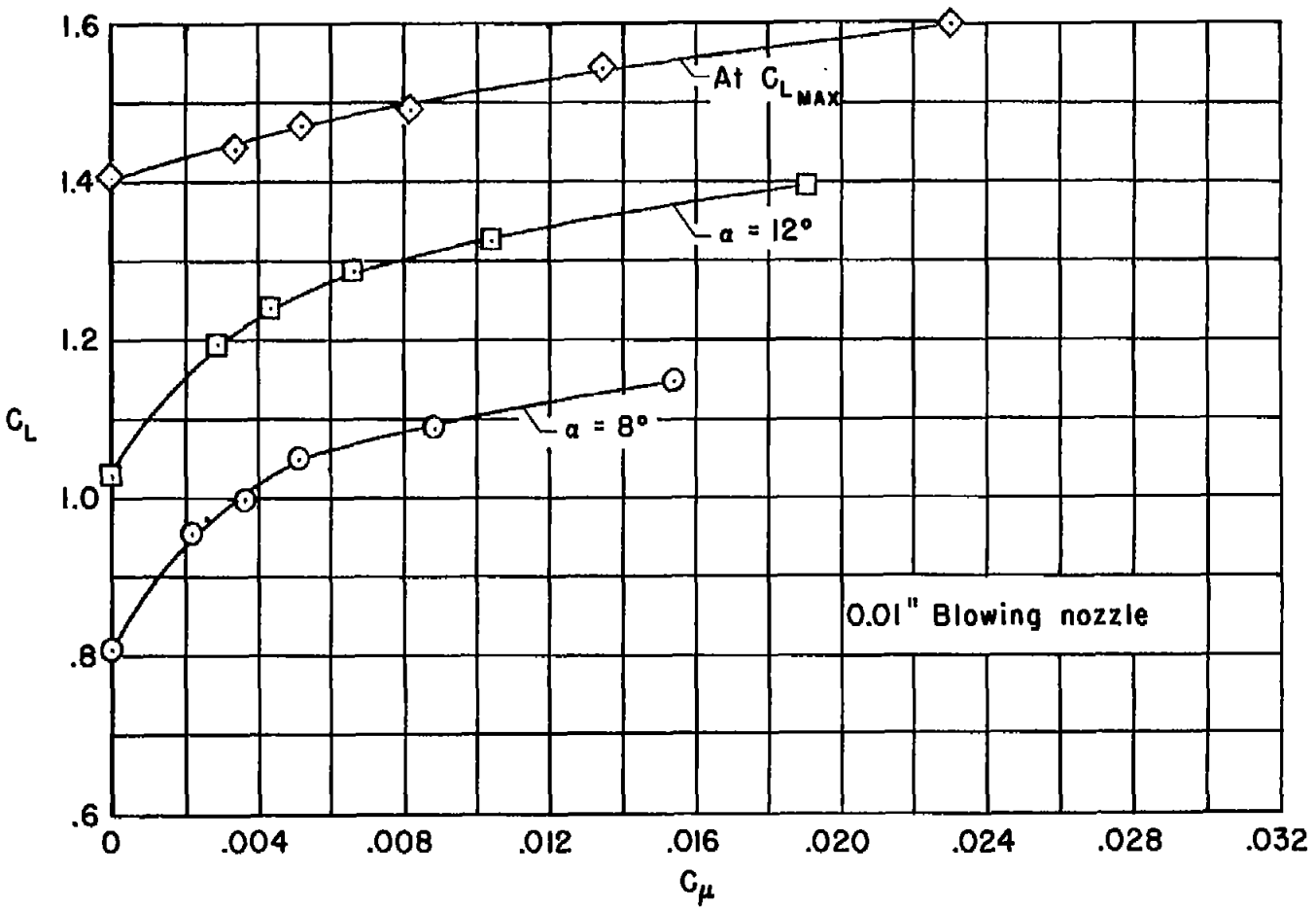

(a) Slatted leading edge.

Figure 25.- Variation of lift coefficient with momentum coefficient; $\delta_f = 55^\circ$.

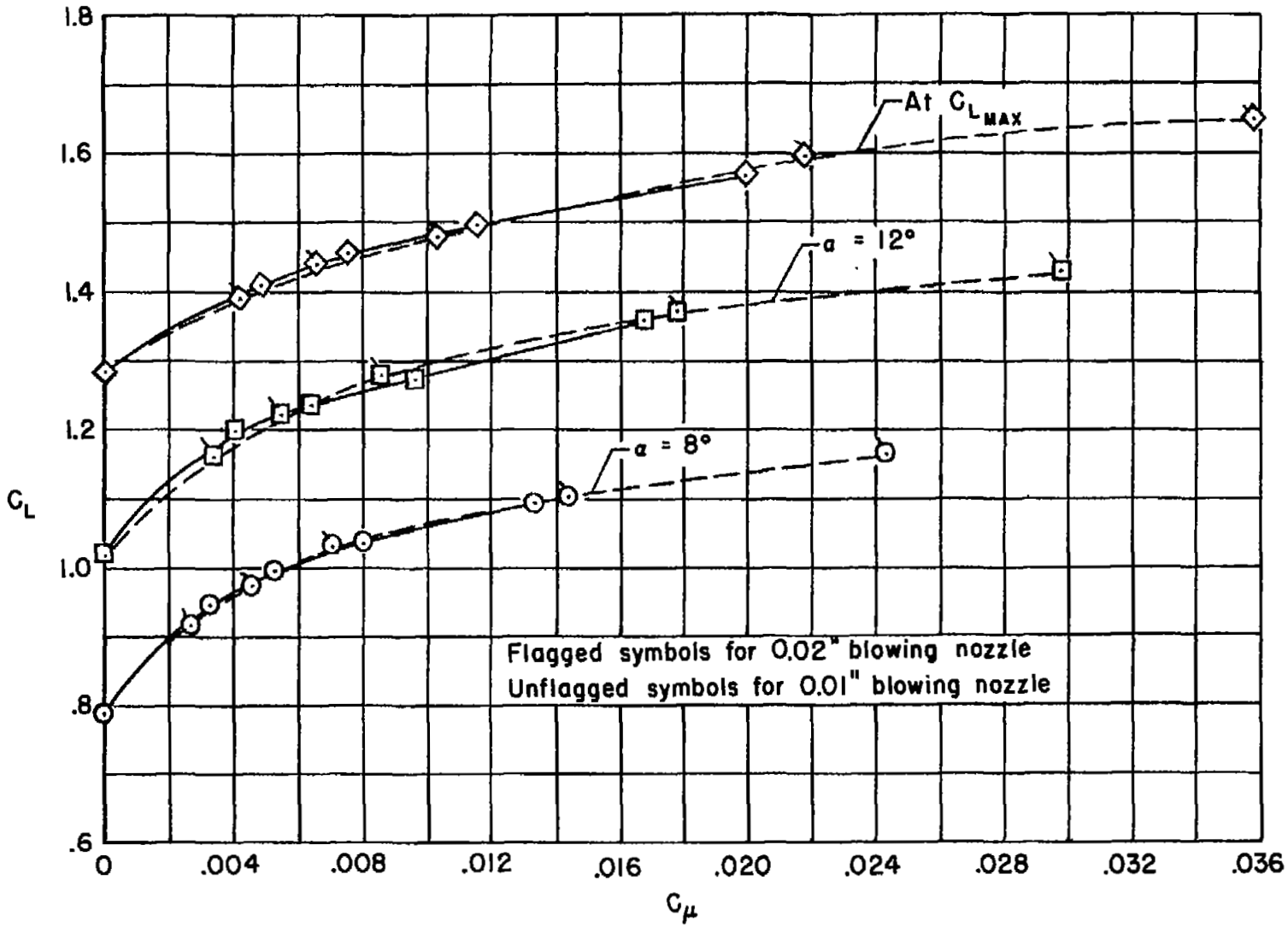

(b) Cambered leading edge.

Figure 25.- Concluded.

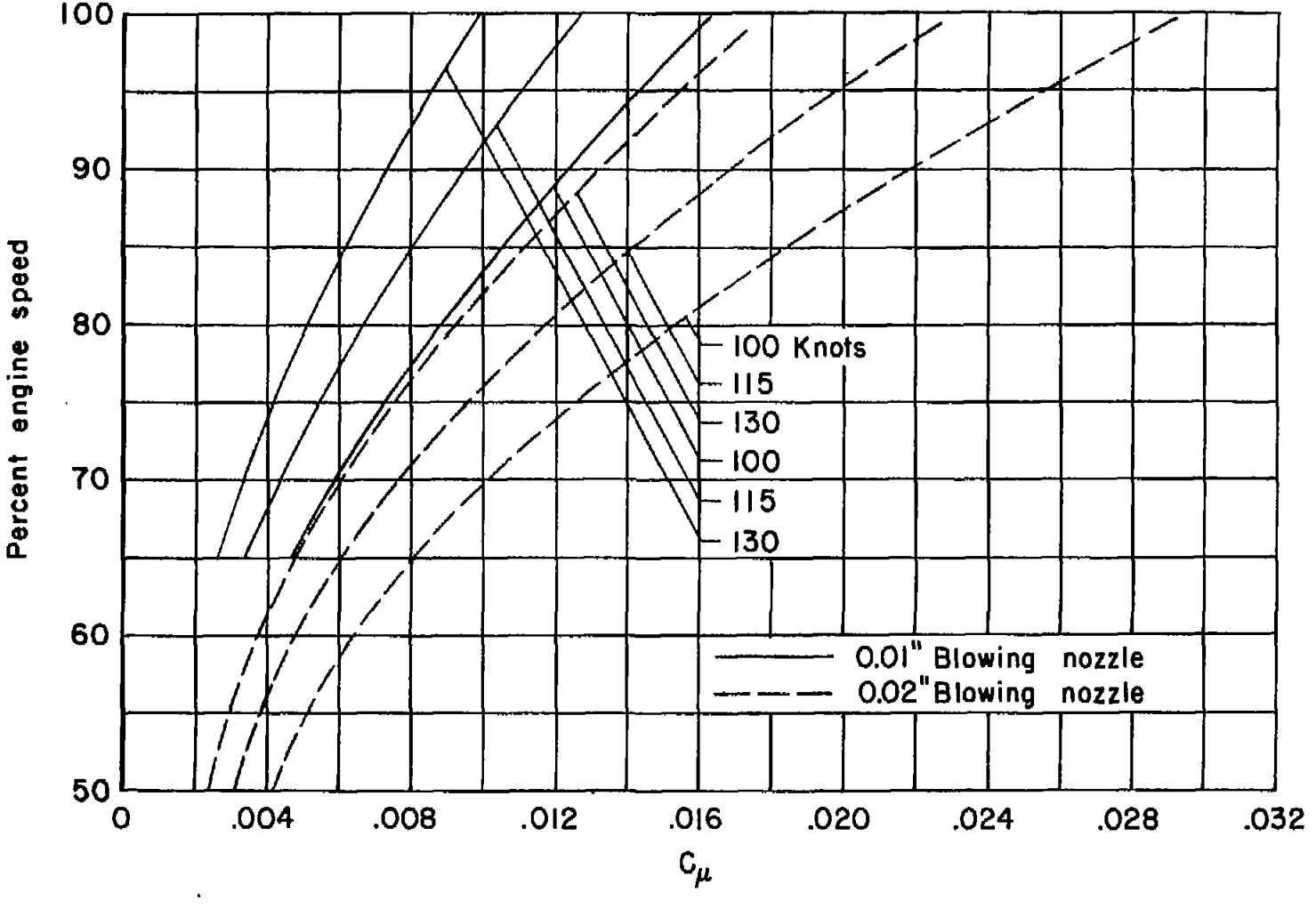

Figure 26.- Variation of momentum coefficient with engine speed.

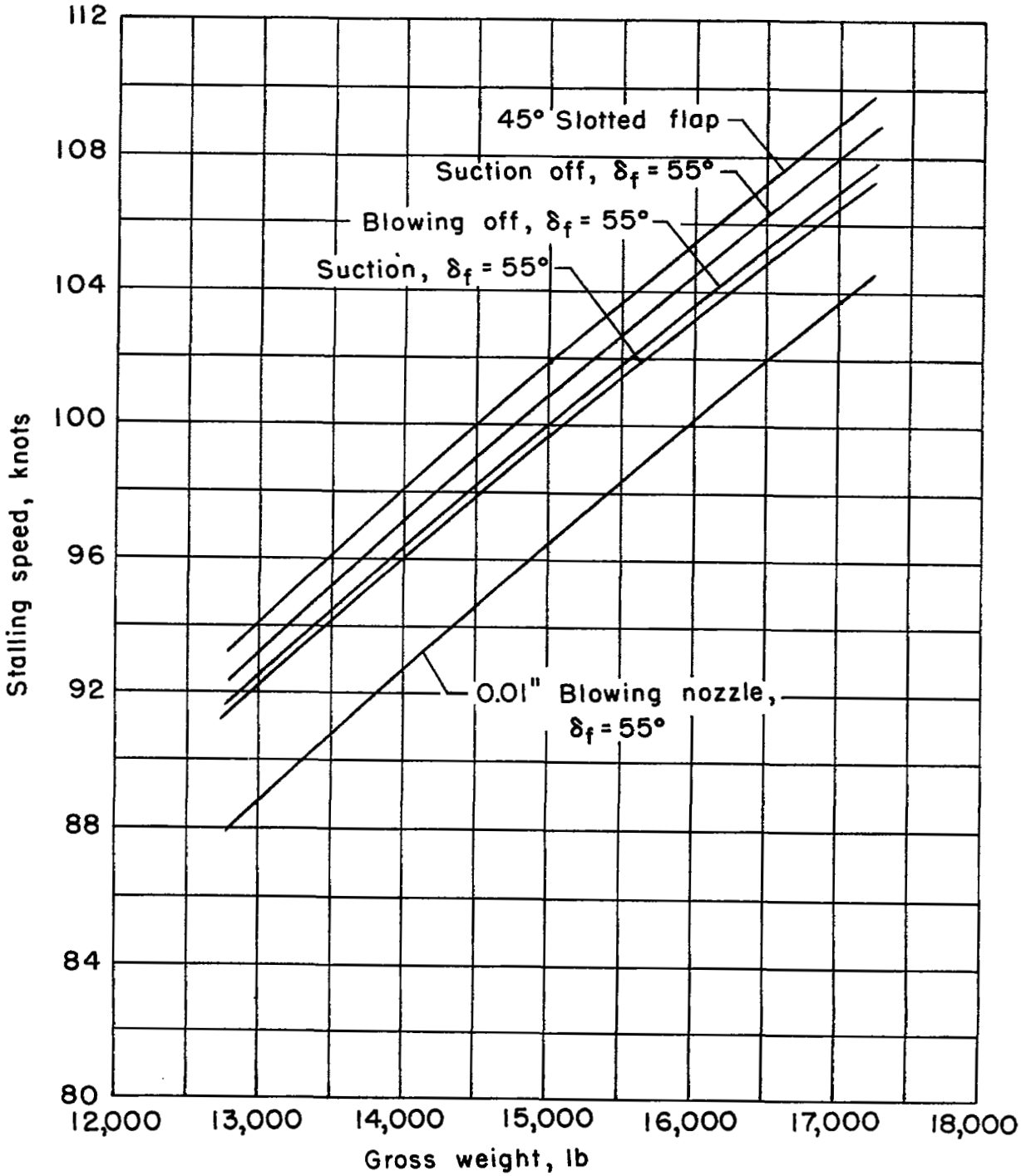

(a) Slatted leading edge.

Figure 27.- Variation of stalling speed with gross weight.

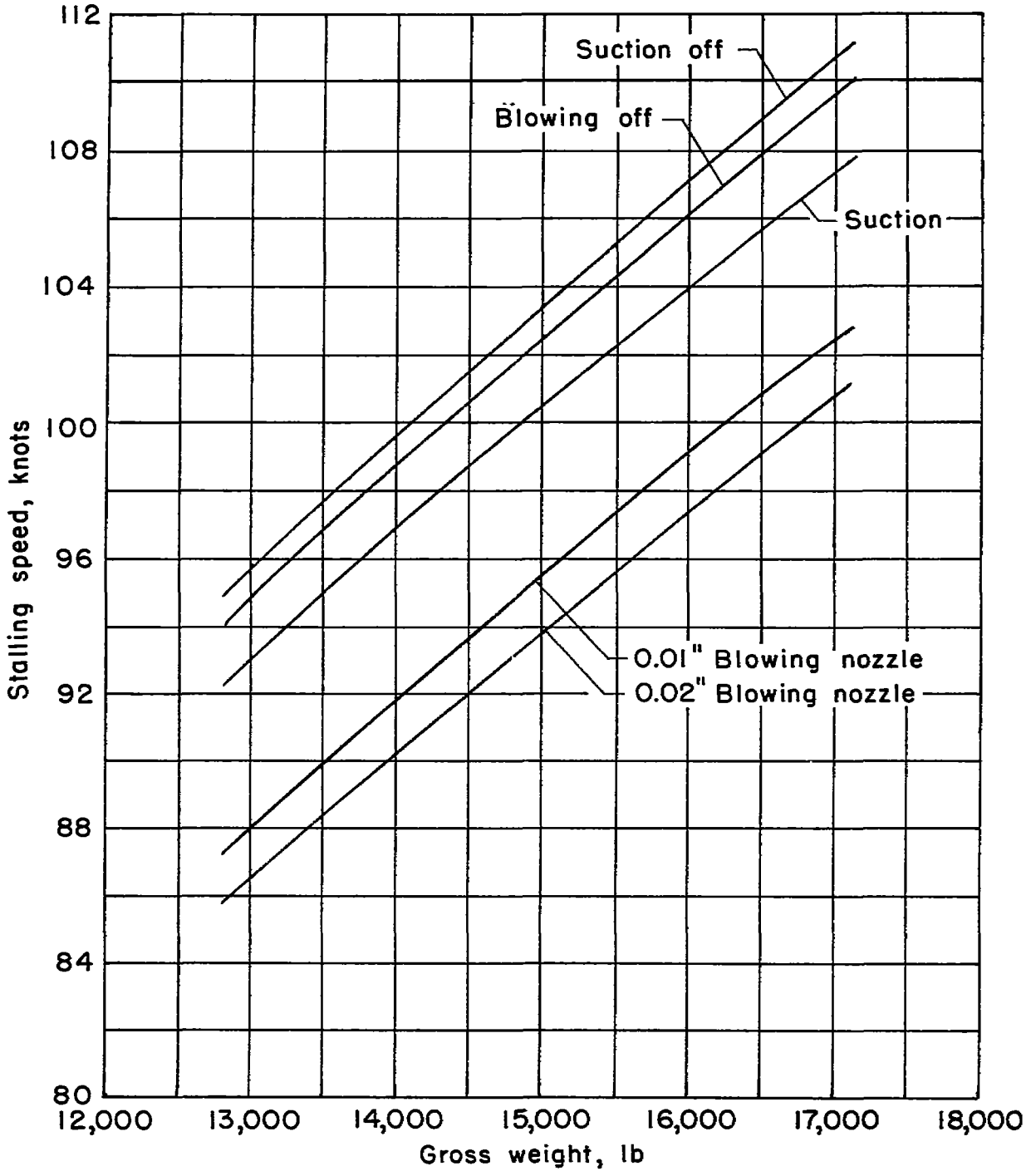

(b) Cambered leading edge; $\delta_f = 55^\circ$.

Figure 27.- Concluded.

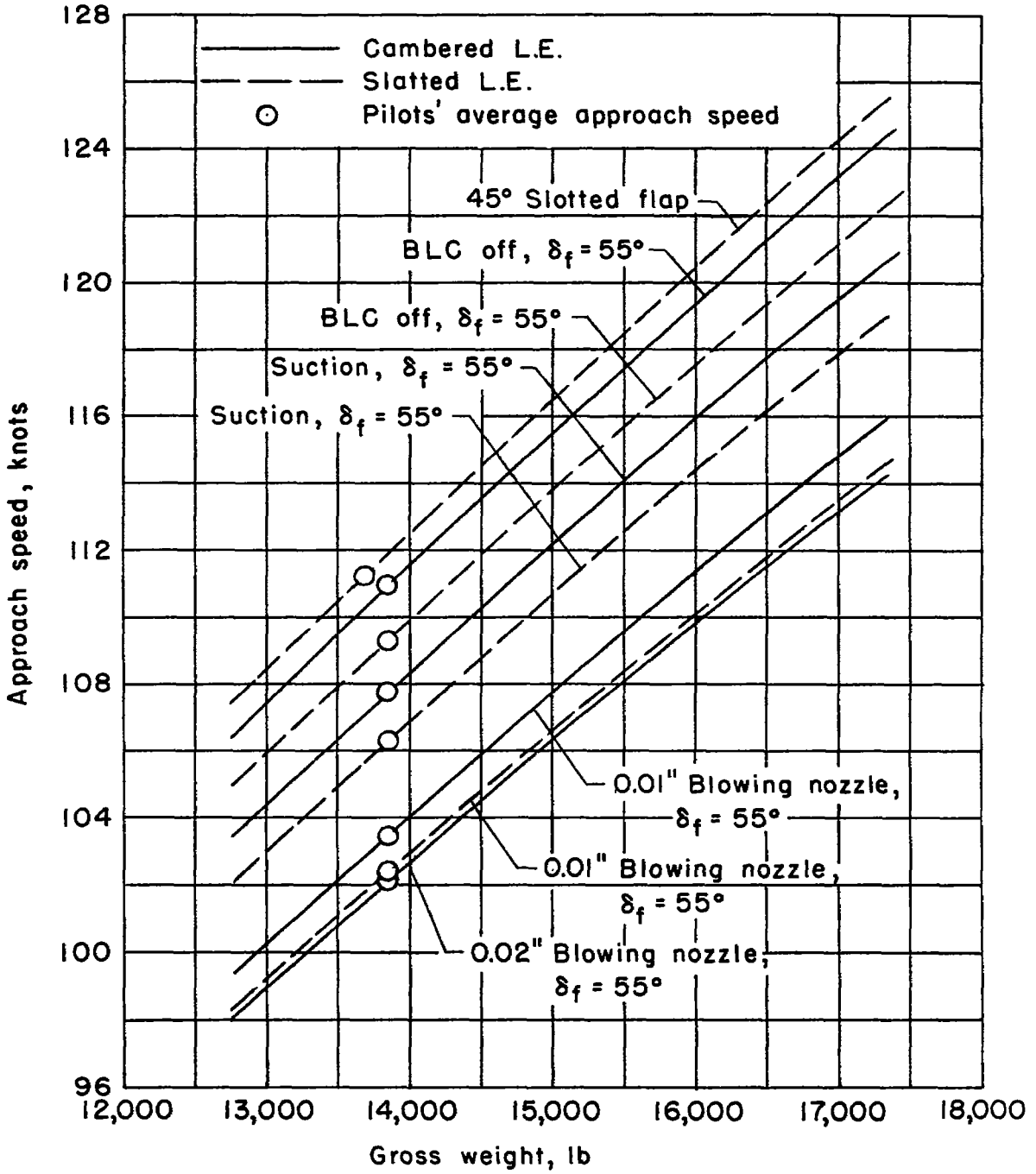

Figure 28.- Variation of approach speed with gross weight.

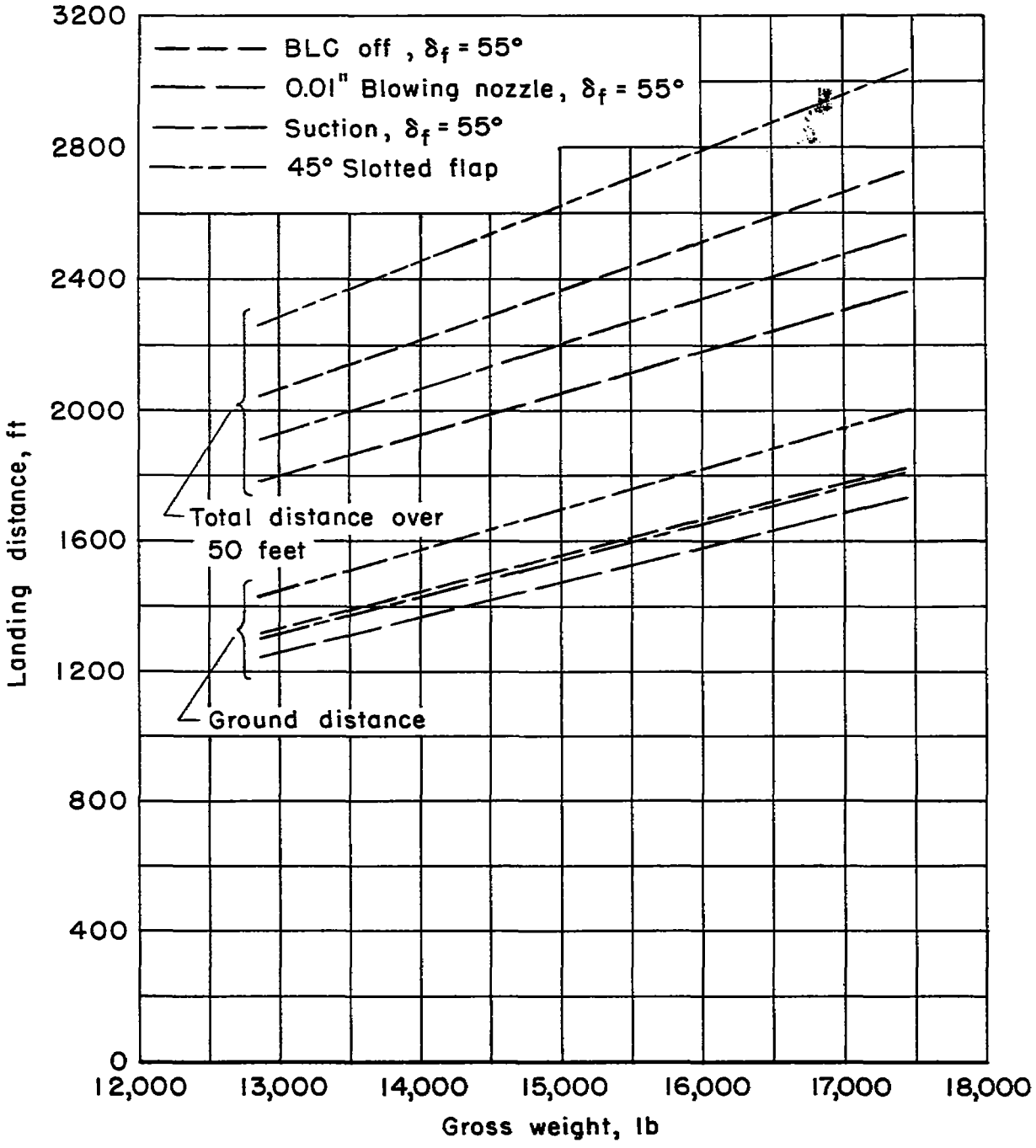

(a) Slatted leading edge.

Figure 29.- Variation of landing distance with gross weight.

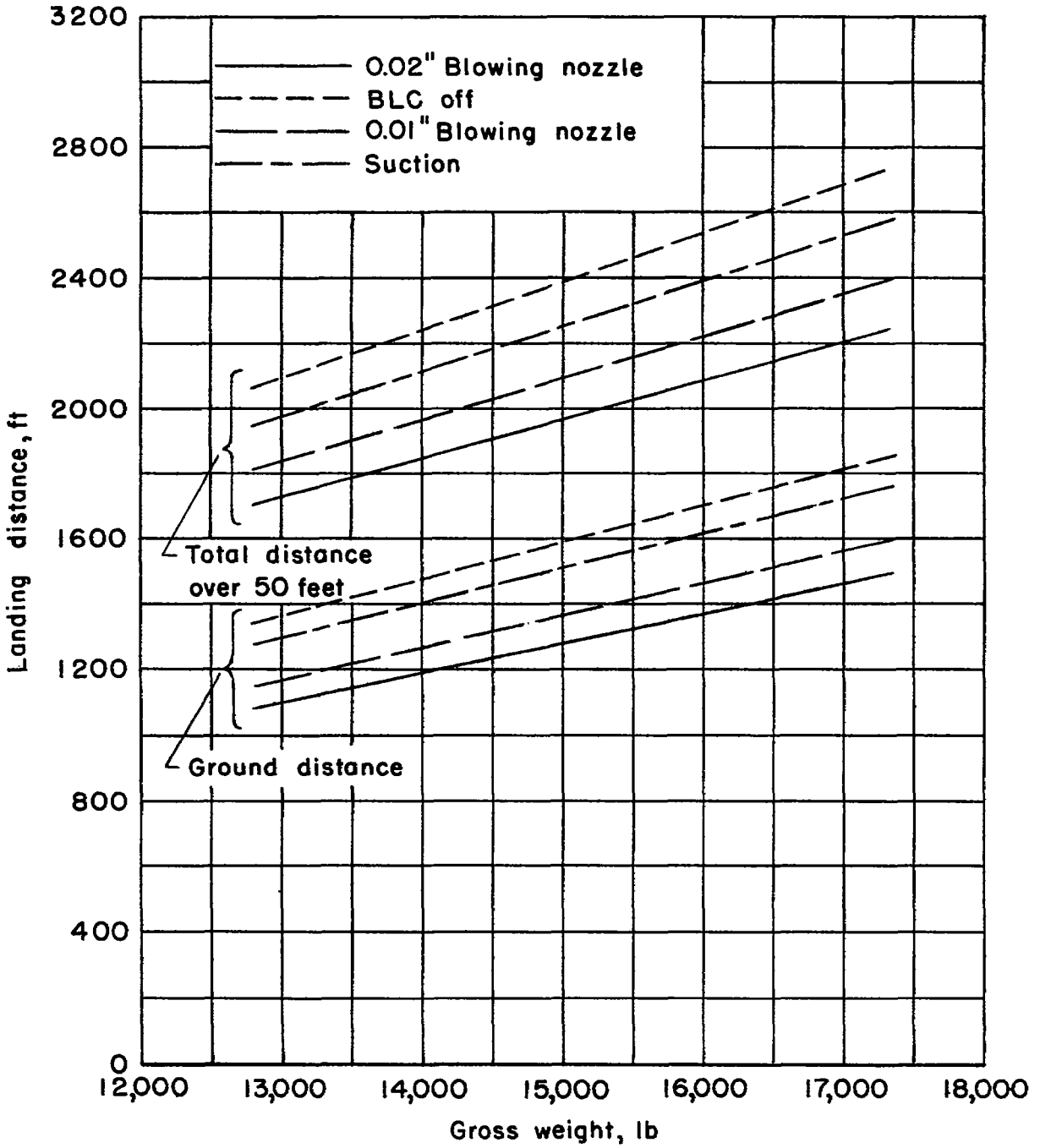

(b) Cambered leading edge; $\delta_f = 55^\circ$.

Figure 29.- Concluded.

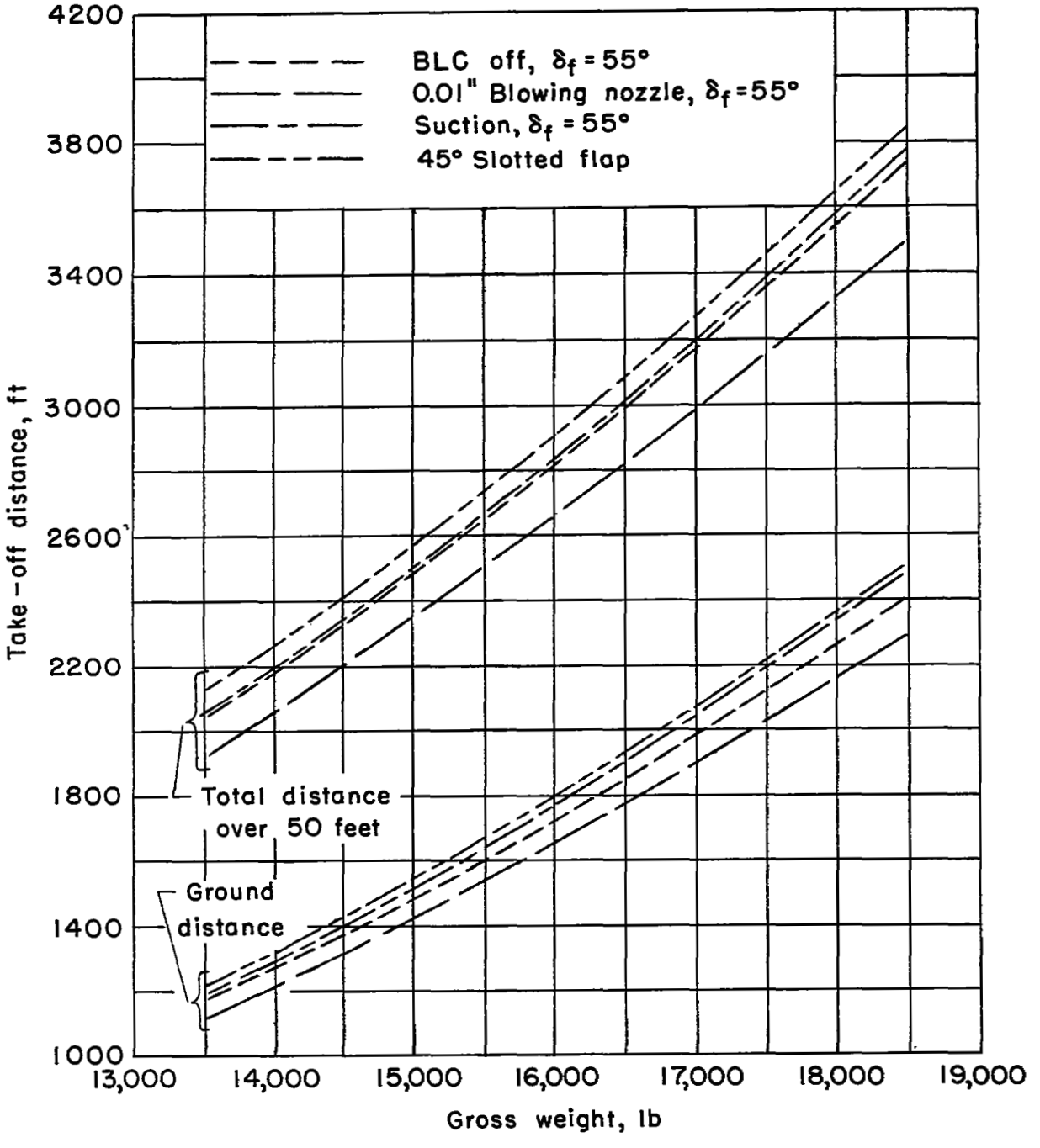

(a) Slatted leading edge.

Figure 30.- Variation of take-off distance with gross weight.

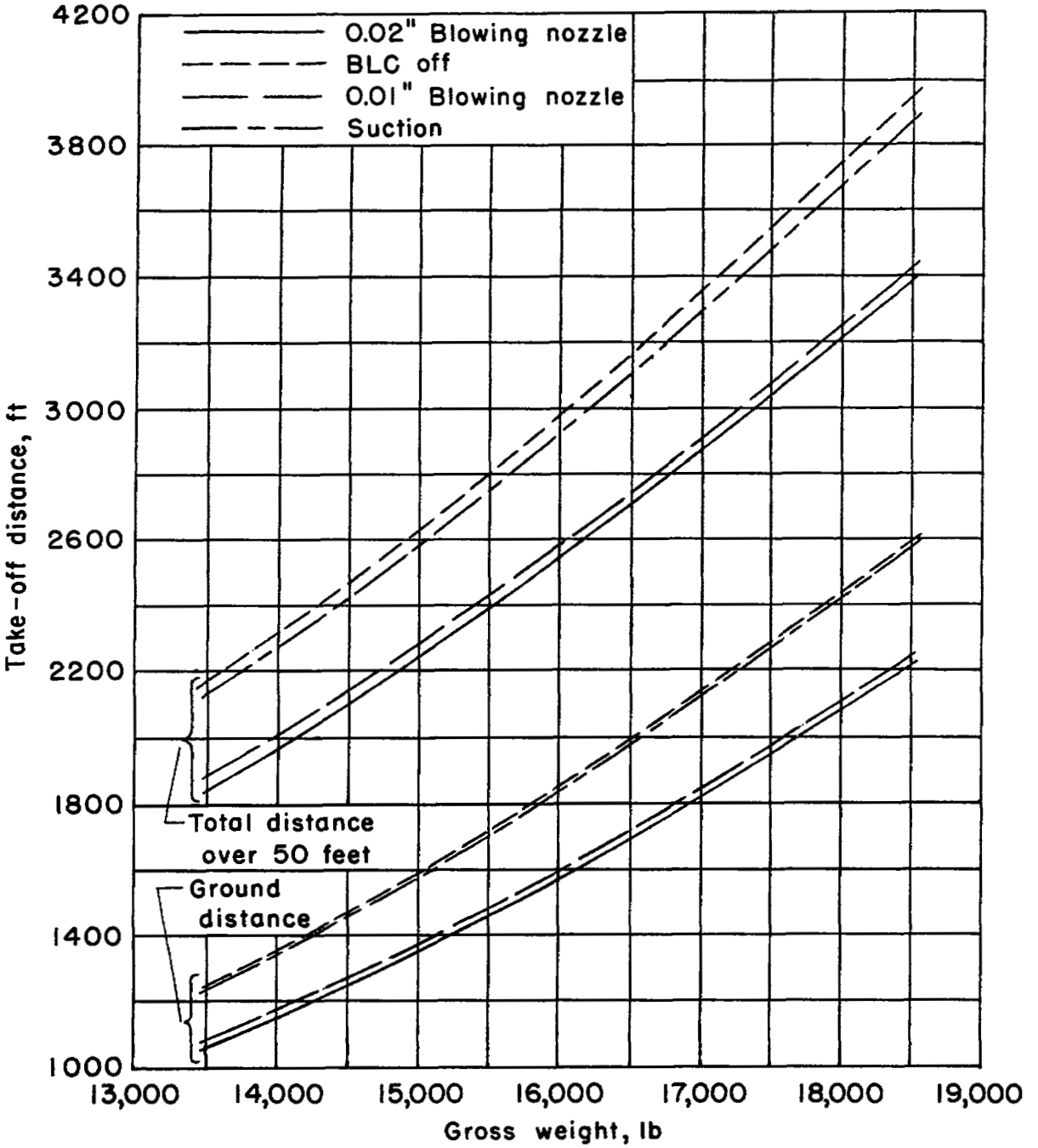

(b) Cambered leading edge; $\delta_f = 55^{\circ}$.

Figure 30.- Continued.

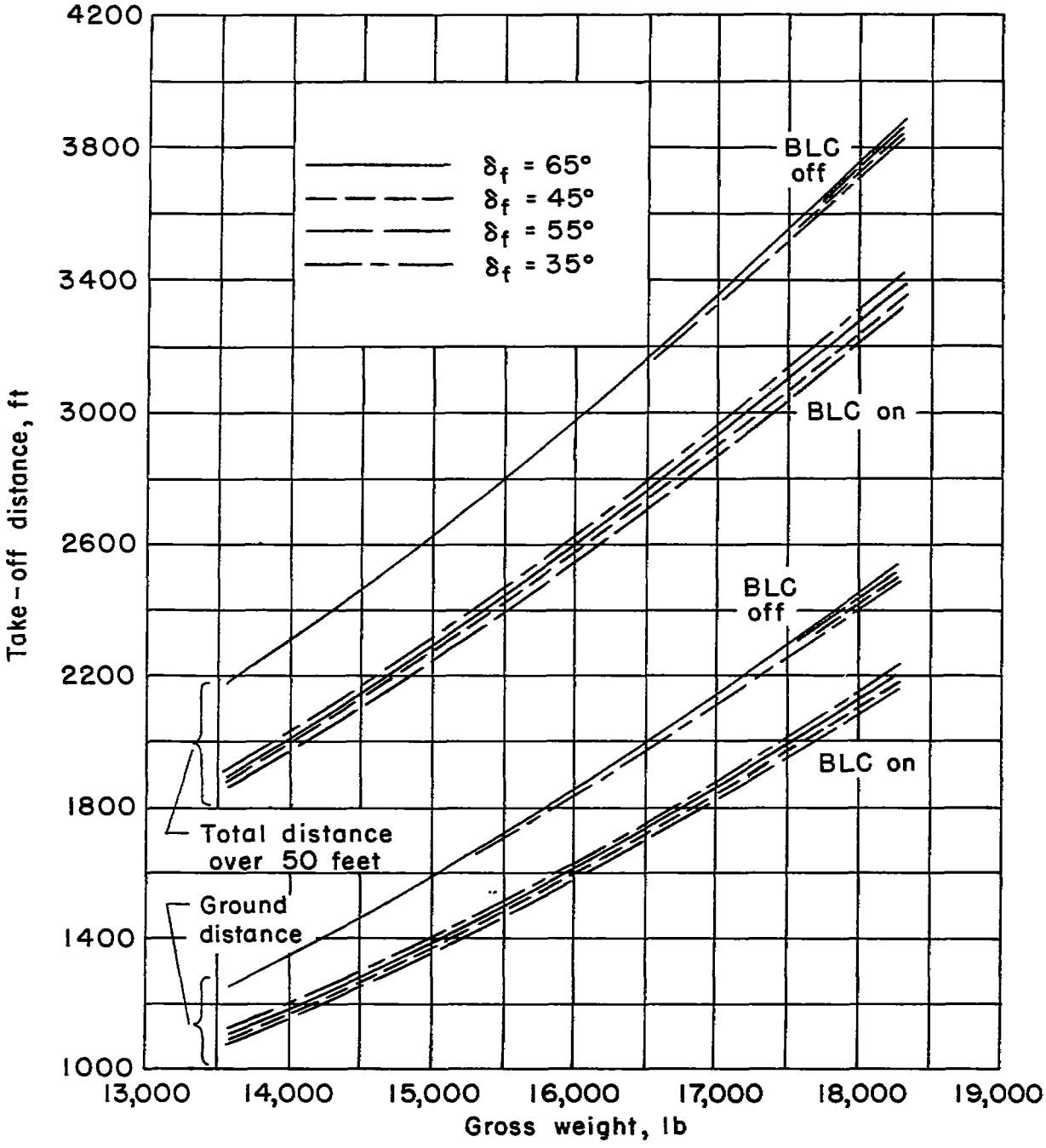

(c) Cambered leading edge; 0.02-inch blowing nozzle.

Figure 30.- Concluded.

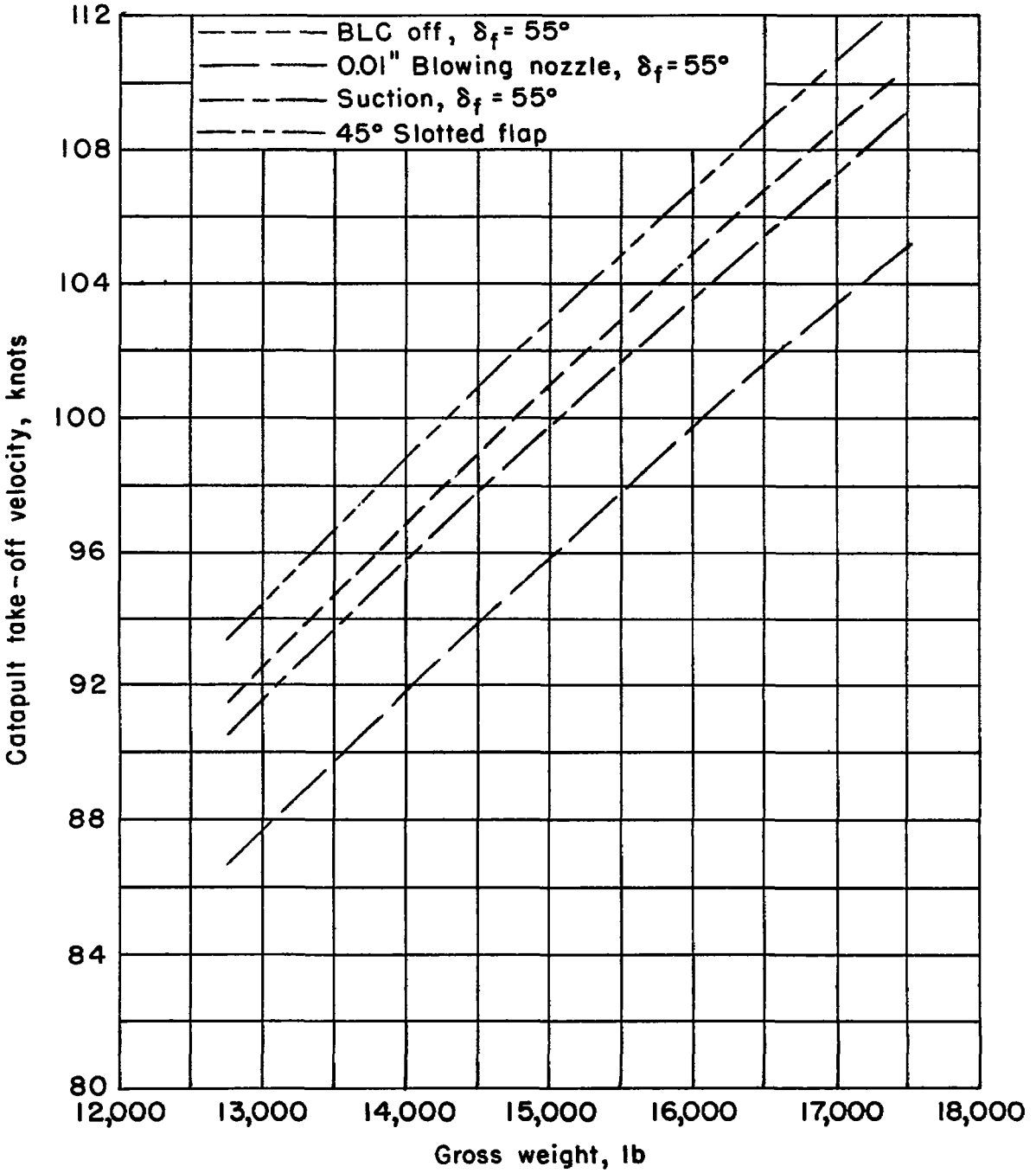

(a) Slatted leading edge.

Figure 31.- Variation of catapult take-off speed with gross weight for various configurations.

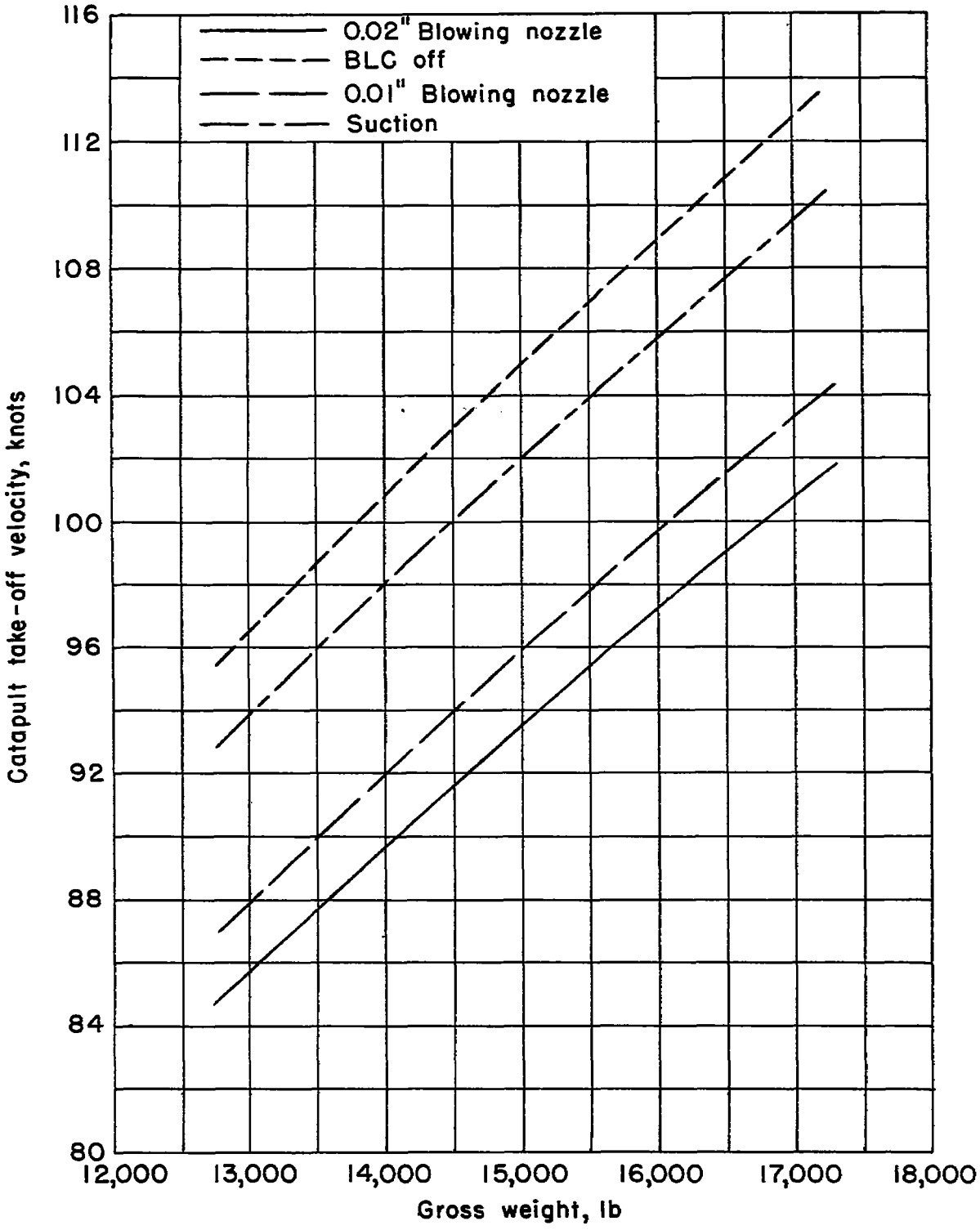

(b) Cambered leading edge; $\delta_f = 55^{\circ}$.

Figure 31.- Concluded.

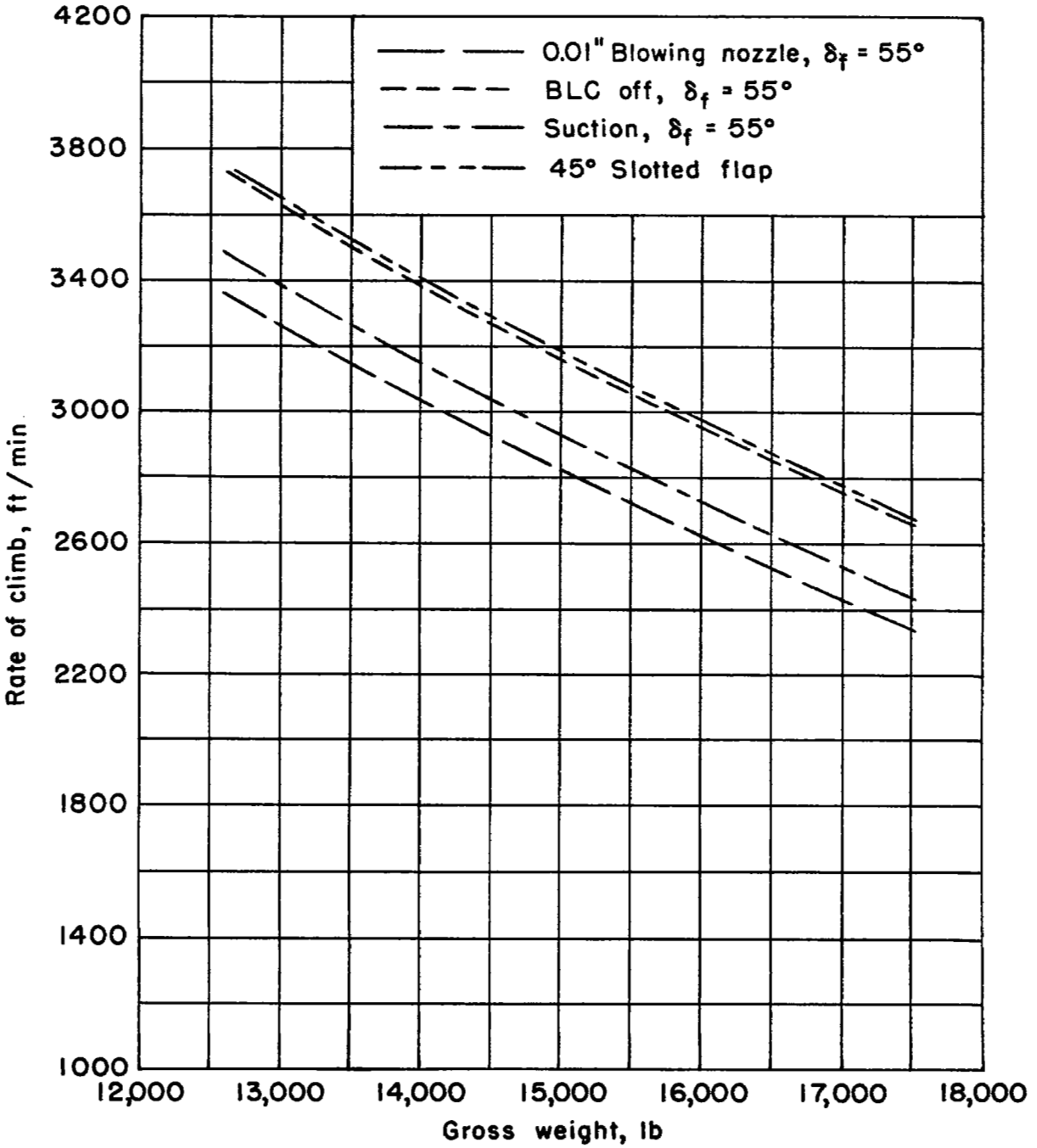

(a) Slatted leading edge.

Figure 32.- Variation of rate of climb with gross weight; climb speed = 1.05 V_S.

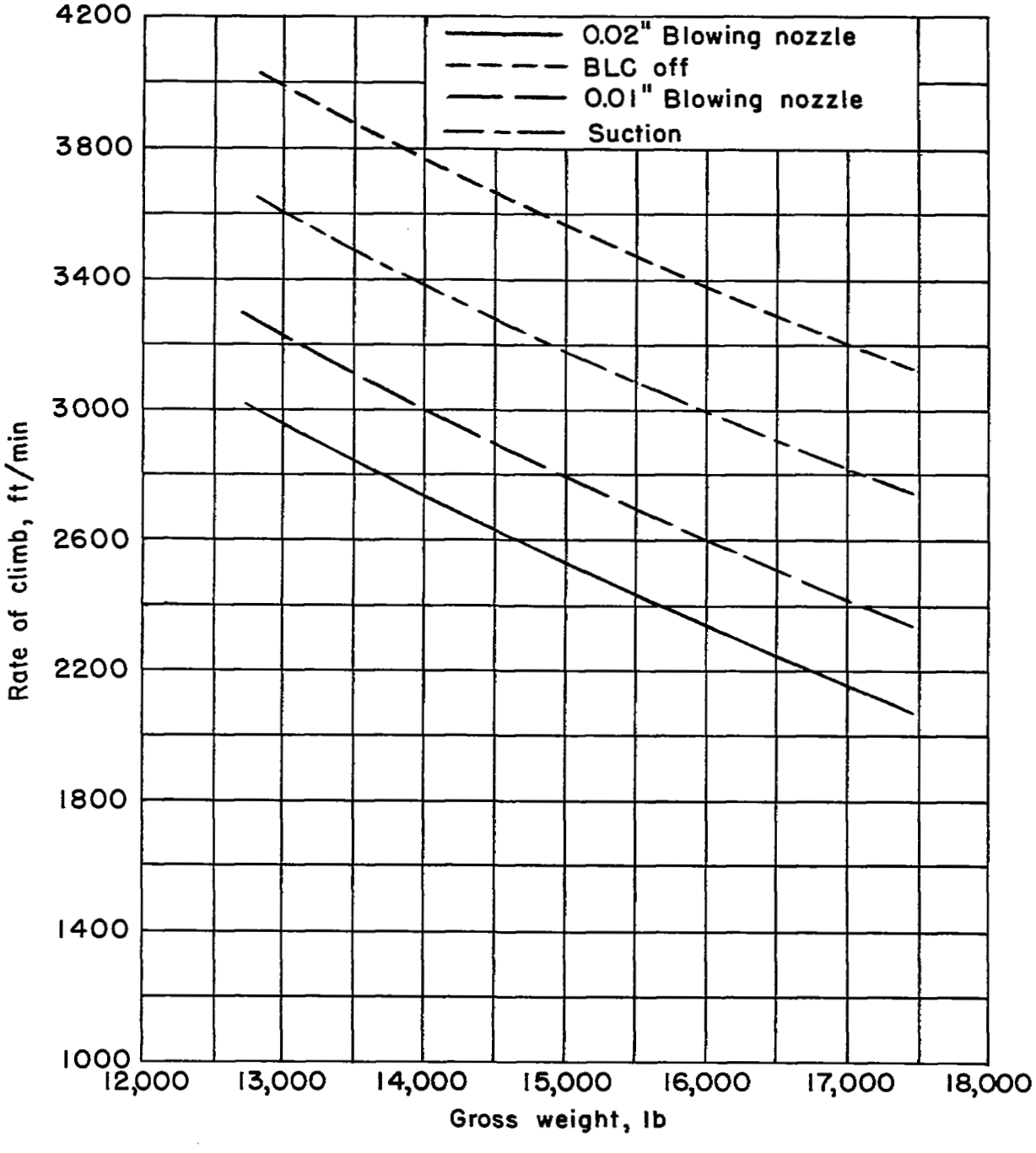

(b) Cambered leading edge; $\delta_f = 55^{\circ}$.

Figure 32.- Concluded.

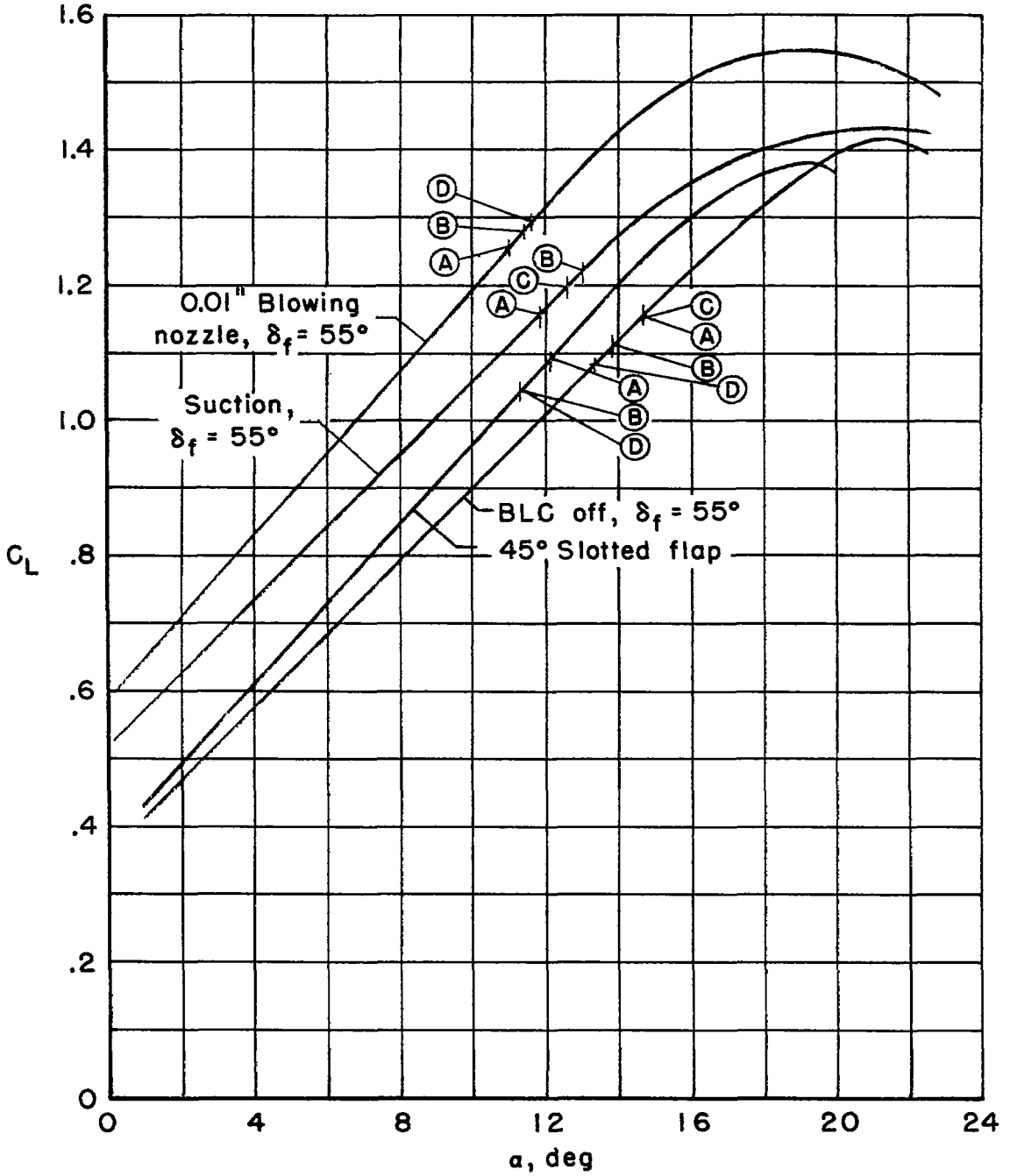

(a) Slatted leading edge.

Figure 33.- Relation of pilots' approach speed to lift curves.

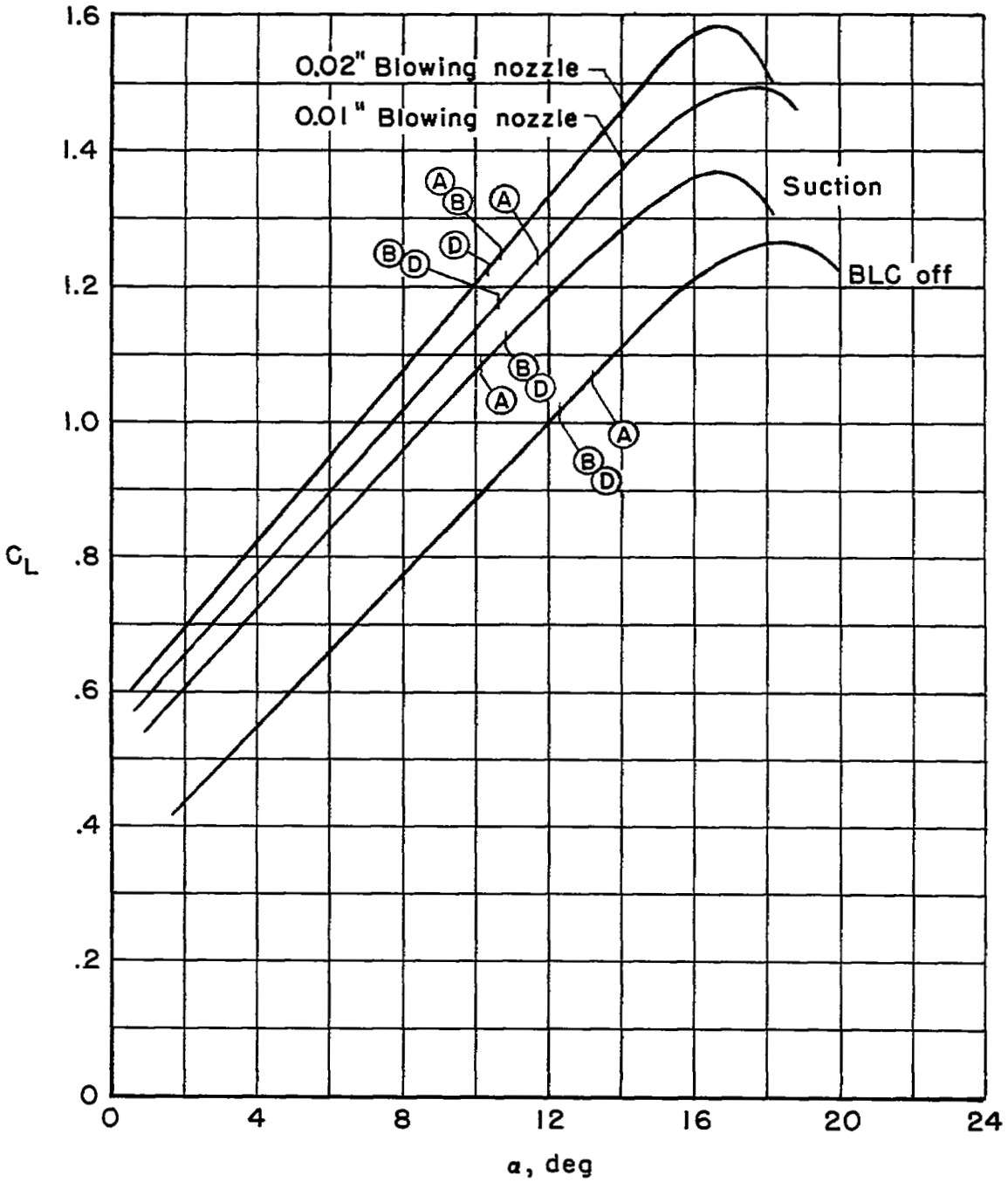

(b) Cambered leading edge; $\delta_f = 55^{\circ}$.

Figure 33.- Concluded.

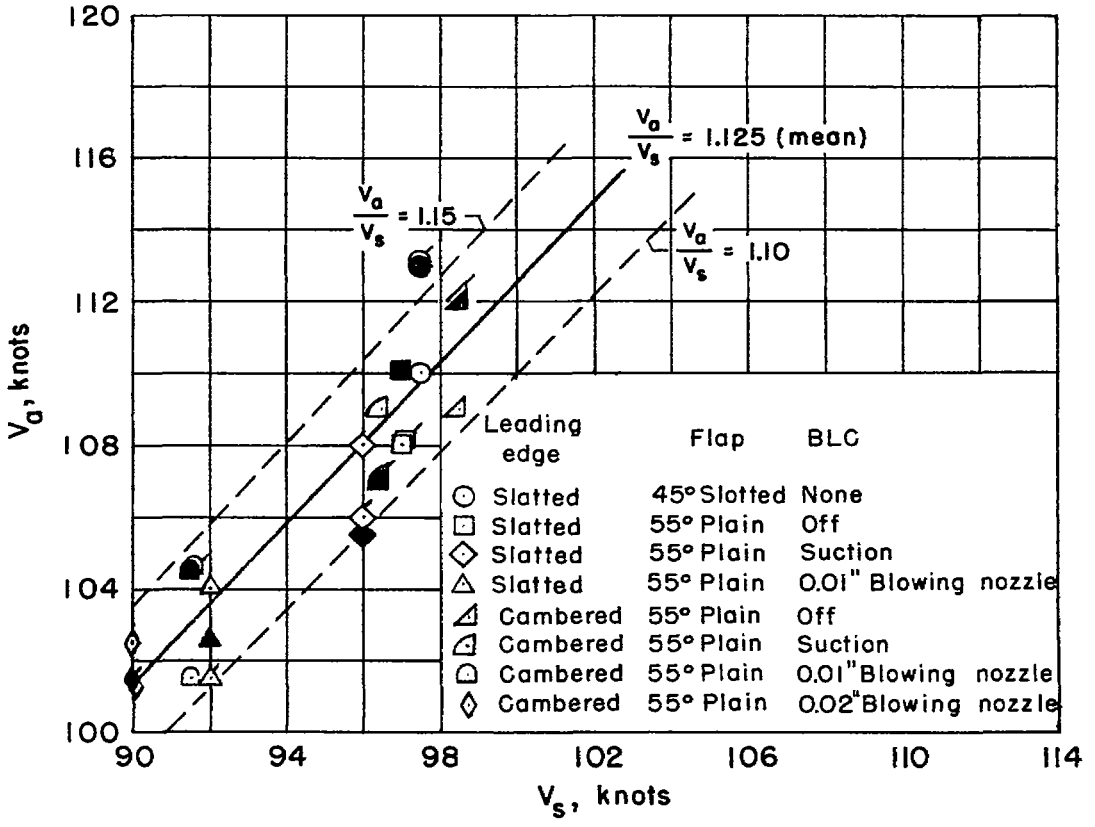

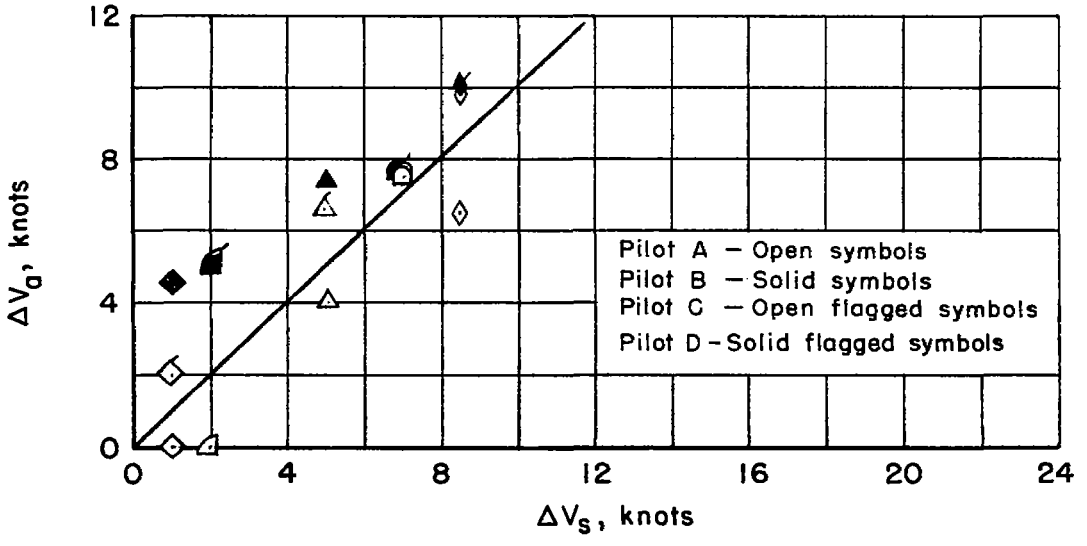

Figure 34.- Variation of approach speed with stall speed.

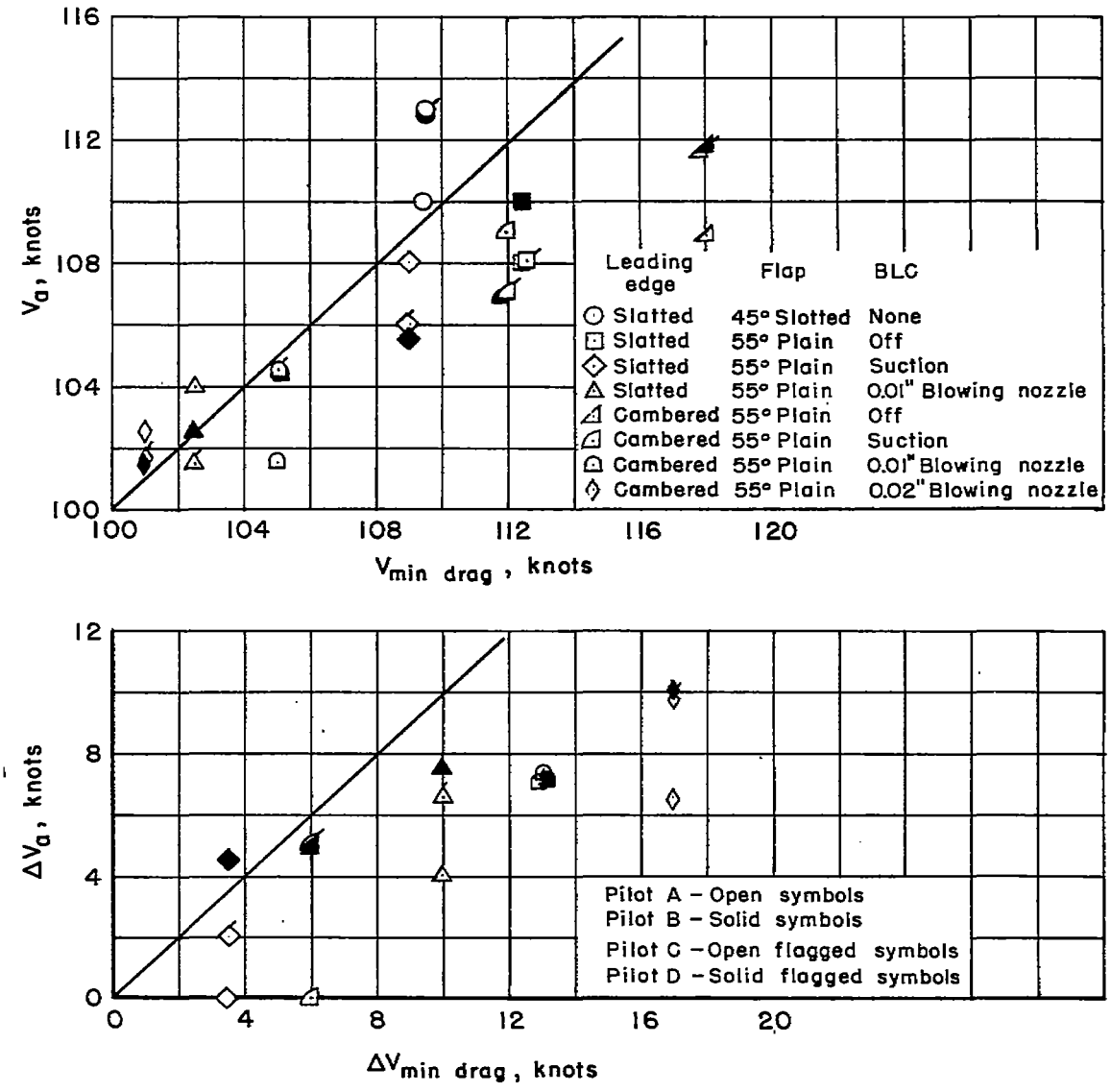

Figure 35.- Variation of approach speed with speed for minimum drag.

NACA - Langley Field, Va.

3 1176 01434 9378